3. RESULTATS

3.1 Cartografia física de marcadors procedents de quatre regions cromosòmiques del braç 3R de *D. melanogaster* a *D. repleta* i *D. buzzatii*

Un dels objectius d'aquest treball era la clonació i caracterització molecular dels punts de trencament d'alguna inversió cromosòmica polimòrfica de *D. buzzatii*. La condició principal per poder-ho fer és disposar d'algun marcador cartografiat prop d'un dels dos punts de trencament de la inversió. La primera part d'aquest treball ha consistit en la cerca d'un marcador que complís aquesta condició. Es disposava de marcadors cartografiats prèviament prop dels punts de trencament de les inversions $2q^7$ i $2z^3$. El gen *Rb97D* i els cosmidis 58B10 i 59B4 s'havien cartografiat prop del punt de trencament distal de la inversió $2q^7$(Ranz *et al*. 1999; Ranz *et al*. 2001). Prop dels extrems de la inversió $2z^3$ s'havien cartografiat els gens *Antp* i *α-Est3* i *α-Est-10*, al punt de trencament proximal, i el bacteriòfag P1 DS08785, al punt de trencament distal. Aquests marcadors es van hibridar sobre cromosomes portadors de les inversions per determinar si estaven dins o fora d'elles. Posteriorment es van hibridar altres marcadors cartografiats prop d'aquests a *D. melanogaster* per comprovar si aquests seguien localitzant-se prop dels punts de trencament. Si els nous marcadors canvien la seva posició relativa respecte a la inversió (dins o fora) significa que el punt de trencament es troba en un segment conservat entre *D. melanogaster* i *D. buzzatii*. En aquest cas és molt possible trobar algun marcador que contingui el punt de trencament o estigui suficientment a prop per permetre la seva clonació mitjançant genoteques de bacteriòfags λ.

La comparació de la posició d'aquests marcadors entre les diferents espècies també ha permès estudiar l'evolució cromosòmica entre *D. melanogaster* i el grup *repleta*. Els marcadors es van cartografiar a *D. buzzatii* i a *D. repleta*, l'espècie de referència del grup. Concretament s'ha analitzat l'organització molecular a *D. repleta* i *D. buzzatii* de tres regions cromosòmiques de *D. melanogaster*. D'aquestes regions provenen els marcadors prèviament localitzats a prop dels punts de trencament de les inversions $2q^7$ i $2z^3$: 83E1-84E1 (*Antp* i *α-Est3*/*10*), 86A4-E2 (DS08785) i 97B1-E6 (*Rb97D*). La regió 95A1-96A23 (58B10 i 59B4) s'havia estudiat prèviament (Ranz *et al*. 1999) i els nous marcadors s'han utilitzat només per a la clonació dels punts de trencament de la inversió $2q^7$. En aquesta regió també s'han utilitzat bacteriòfags P1 d'una genoteca de *D. virilis* (Lozovskaya *et al*. 1993; Vieira *et al*. 1997b).

Els marcadors cartografiats en aquest treball s'han utilitzat juntament amb els cartografiats prèviament per altres membres del grup d'investigació per elaborar un mapa d'alta densitat del cromosoma 2 de *D. repleta*, i comparar la seva organització amb la del braç cromosòmic 3R de *D. melanogaster*. Els resultats es van publicar a la revista *Genome Research* (volum 11, pàgines 230-239) amb el títol: **How malleable is the eukaryotic genome? Extreme rate of chromosomal rearrangement in the genus *Drosophila*** (annex 1).

3.1.1 Hibridacions control

Totes les hibridacions control, excepte la del gen *ro,* s'han realitzat sobre preparacions cromosòmiques de *D. melanogaster*, la seva espècie de procedència. A la Figura 6a es mostra la hibridació control de tres marcadors. La hibridació control per al gen *ro* s'ha dut a terme sobre una preparació cromosòmica de *D. virilis* (Figura 6m). Dels 61 clons hibridats, 49 van donar un senyal únic que coincidia aproximadament amb la informació prèvia disponible sobre la seva localització física (Taula 9). Tot i això, per a la majoria de clons s'ha canviat lleugerament la seva posició. En molts casos s'ha augmentat la precisió en la localització dels clons, però la nova posició que proposem està inclosa dins dels marges de l'anterior. Només en una ocasió s'ha assignat un marcador a una divisió diferent. És el cas del bacteriòfag P1 DS08128, localitzat anteriorment a la banda 84E1-2, i que s'ha localitzat en aquest treball a la banda 83E1-2. La posició de quatre clons més (DS00184, *Ppp*, DS04173 i 58A3) tampoc coincideix amb la que apareix a la literatura, però en aquests casos la nova posició que proposem és molt propera a l'anterior. Finalment, alguns marcadors van produir més d'un senyal d'hibridació. El bacteriòfag P1 DS00464 va produir dos senyals d'hibridació d'igual intensitat, una a cada costat de la banda 83C1-2. Davant la impossibilitat d'assignar-li una posició exacta es va utilitzar el clon DS08010, que prové de la mateixa regió, dóna un sol senyal en els cromosomes de *D. melanogaster* i mostra la mateixa homologia en les espècies del grup *repleta*. Per altra banda sis bacteriòfags P1 (DS00263, DS06359, DS00619, DS04424, DS07662 i DS06282) van donar lloc a varis senyals d'hibridació en diferents cromosomes. En el cas de DS00619, DS04424, DS07662 i DS06282, tot i que produeixen senyals múltiples, es pot apreciar un senyal de major intensitat a bandes que coincideixen amb la seva localització prèvia. Els senyals múltiples no van

desaparèixer en realitzar la hibridació augmentant la temperatura (42ºC) o sobre els cromosomes d'una soca diferent de *D. melanogaster* (Oregon R).

3.1.2 Hibridacions heteròlogues

3.1.2.1 Hibridacions heteròlogues positives

Les hibridacions sobre *D. buzzatii* s'han fet sobre cromosomes portadors de les inversions $2q^7$ (clons procedents de les regions 95A1-96A23 i 97B1-E6) i $2z^3$ (clons procedents de les regions 83E1-84E1 i 86A4-E2). 54 dels 59 clons que es van hibridar sobre els cromosomes de *D. buzzatii* van donar un resultat positiu. Totes les sondes van hibridar en el cromosoma 2 excepte en el cas de DS05426, que va donar un senyal en el cromosoma 2 i un secundari en el cromosoma X. D'aquests 54 clons se'n van triar 14 per ser hibridats sobre els cromosomes de *D. repleta*. Tots van donar resultats positius. Un clon, el bacteriòfag P1 DS06282 no s'ha hibridat sobre *D. buzzatii*, però va donar resultat positiu en hibridar-lo sobre cromosomes de *D. repleta*. El gen *α-Est1* no s'ha hibridat a les espècies del grup *repleta* degut a què ja s'havien cartografiat prèviament els gens *α-Est3* i *α-Est10*, situats en el mateix *cluster* de gens (Ranz *et al*. 2001). A més, marcadors situats als dos costats del *cluster* hibriden a la mateixa banda a *D. repleta* i *D. buzzatii*. A la Figura 6 es mostren alguns exemples d'hibridacions heteròlogues.

3.1.2.2 Hibridacions heteròlogues negatives

Cinc dels 45 bacteriòfags P1 no van donar cap senyal d'hibridació després de varis intents sobre preparacions de *D. buzzatii*. Aquests fags són el següents: DS00263, DS06951, DS04651, DS00758 i DS06359. El bacteriòfag P1 DS06951 també va donar resultat negatiu en hibridar-lo sobre els cromosomes de *D. repleta*.

El gen *ro*, procedent de *D. virilis*, no va donar cap senyal en ser hibridat sobre els cromosomes de *D. melanogaster*, però la seva localització és coneguda (Heberlein i Rubin 1990).

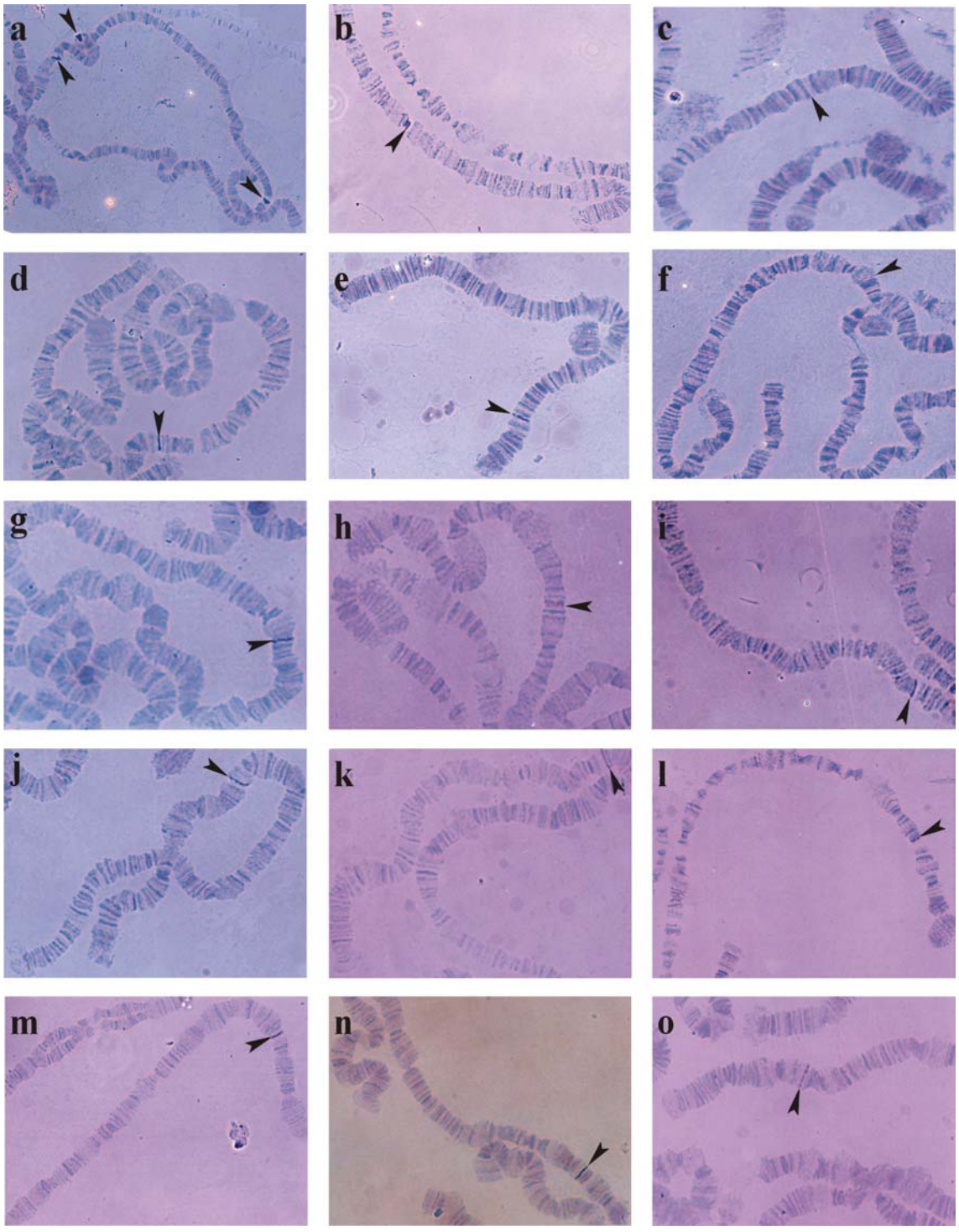

Figura 6. Fotografies de les hibridacions: (a) DS08128/DS02384/172D2 sobre *D. melanogaster*, (b) DS00276 sobre $2jz^3$, (c) DS08010 sobre *D. repleta*, (d) DS05661 sobre $2jz^3$, (e) DS05661 sobre *D. repleta*, (f) DS04597 sobre $2jz^3$, (g) DS02168 sobre $2jz^3$, (h) DS07442 sobre $2jq^7$, (i) DS05188 sobre $2jq^7$, (j) DS06282 sobre *D. repleta*, (k) DS00238 sobre $2jq^7$, (l) *ro* sobre $2jq^7$, (m) *ro* sobre *D. virilis*, (n) Dv1424 sobre *D. virilis*, (o) *T48* sobre $2jq^7$.

Taula 9. Resultats de les hibridacions homòlogues i heteròlogues.

Sonda	***D. melanogaster***		***D. buzzatii***	***D. repleta***
	Literatura	**Aquest treball**		
DS08128 [c]	84E1-2	83E1-2	C2e	ND
DS05926 [c]	83F1-2	83F1-2	D5a	D5a
DS07437 [c]	83F1-2	83F2-84A1	D5a	D5a
DS00263 [c]	83F1-2	Múltiples	-	ND
DS00276 [c]	84A4-5	84A4-5	F1c-e	ND
DS07700 [c]	83F1-84B2	83B1-3	F1c	ND
DS00464 [c]	84B2-C2	84B4-6/84C4-6	C7e	ND
DS06951 [c]	84B2-C2	84B2-C2	-	-
DS08010 [c]	84C1-6	84C1-6	C7e	C7e
DS00184 [c]	84D1-2	84C7-8	C7e/F5e	C7e/F5e
DS04025 [c]	84D1-2	84C7-8	F5e	ND
DS06617 [c]	84D1-2	84D1-2	F5e	ND
DS04651 [c]	84D1-10	84D1-10	-	ND
α-Est1 [a]	84D3-10	84D8-10	ND	ND
DS00538 [c]	84D9-10	84D10-12	F5e-F6a	F5e-6a
DS05426 [c]	84D12-14	84D13-14	F5e / XH1a	F5e
DS06961 [c]	86A5-B2	86B1-2	F6f	F6f
DS00758 [c]	86B1-6	86B1-6	-	ND
DS06359 [c]	86A1-F2	Múltiples	-	ND
DS05661 [c]	86C1	86C1	G2d	G2d
DS00618 [c]	86C1-2	86C1-2	G2d	ND
DS00688 [c]	86C1-2	86B4-C1	G2d	ND
DS01137 [c]	86C4-6	86C2-6	G2d	G2d
DS01290 [c]	86C7-8	86C7-8	G4c	ND
DS04597 [c]	86A1-F2	86C7-8	E4a	ND
DS04607 [c]	86C13-15	86C13-15	E4a	ND
DS02384 [c]	86A1-F2	86D5-E1	G3f/C6a-c	ND
DS02168 [c]	86E1-2	86E1-2	C6a-c	C6a-c
DS05515 [c]	95B7-9	95B7-9	D3c-d	ND
DS07442 [c]	95B8-C4	95C1-4	D3c-d	ND
DS00619 [c]	95C1-7	95C1-7/Múltiples	D3c-d	ND

DS04424 [c]	95B1-C7	95C1-7/Múltiples	D3c-d	ND
DS07662 [c]	95B1-C7	95C1-7/Múltiples	D3c-d	ND
Pli [a]	95C5-C8	95C7-9	D3c	ND
DS05188 [c]	95C4-8	95C7-11	D3c	ND
DY852 [d]	95C3-E2	95C1-D9	D3c-d/D1e/A3f/F5e/C6b-c	ND
DS06282 [c]	97B1-2	97B1-3/Múltiples	ND	E3d
DS06669 [c]	97B6-7	97B2-7	E3d/F4c	E3d/F4c
190H12 [b]	97B1-C5	97C1-3	F1h	ND
DS01035 [c]	97C1-D9	97C1-3	F1h	ND
DS00238 [c]	97C1-3	97C1-3	F1h	ND
DS00612 [c]	97C1-3	97C1-3	F1h	ND
Ppp [a]	97D	97C1-3	F1h	F1h*
DS09067 [c]	97C1-D2	97C3-D1	F1h/C4a	ND
DS04173 [c]	97C4-5	97D1-2	C4a	ND
11H12 [b]	97D1-15	97D1-2	C4a	ND
DS05785 [c]	97D1-2	97D1-2	C4a	ND
DS07918 [c]	97D1-2	97D1-2	C4a	C4a*
DS04842 [c]	97D1-2	97D1-2	C4a	ND
DS01238 [c]	97C1-D9	97D1-2	C4a	ND
Tl [a]	97D2	97D1-2	C4a	C4a
DS02698 [c]	97D1-6	97D1-6	C4a	ND
129D7 [b]	97D1-15	97D5-6	D3b-c	ND
ro [a]	97D5	ND	D3b-c	D3b-c*
Rb97D [a]	97D5	97D5	D3b-c	D3b-c*
T48 [a]	97D9	97D9	C2c	C2c*
147A8 [b]	97D1-15	97D12	B3g	ND
167A9 [b]	97E1-11	97E1-6	B3g/B1b	B3g/B1b
115B9 [b]	97E1-11	97E1-6	B3g	ND
58A3 [b]	97D1-15	97E4-6	B3g	B3g
171D2 [b]	97E1-11	97E4-6	B3g	ND

[a]sondes gèniques; [b] cosmidis; [c] bacteriòfags P1; [d] YACs.
ND, no determinat; -, resultat negatiu en la hibridació.
* Cartografiats per Ranz (1998).

3.1.3 Organització molecular de les regions cromosòmiques 83E1-84E1, 86A4-E2 i 97B1-E6 a *D. repleta* i *D. buzzatii*

La Figura 6a mostra la localització sobre el cromosoma 3R de *D. melanogaster* de tres marcadors procedents de les tres regions estudiades. A més dels marcadors cartografiats en aquest treball s'han utilitzat altres marcadors de les mateixes regions de *D. melanogaster*, cartografiats a *D. buzzatii* i *D. repleta* prèviament (Taula 10).

Taula 10. Marcadors cartografiats en altres estudis utilitzats en aquest treball.

Clon	***D. melanogaster***	***D. buzzatii* i *D. repleta***
DS01673 (2)	83 E1-2	C2e
Pak (2)	83E4-6	D2a
Pb (2)	84A5	F1e
DS03540 (2)	84A5	F1c-d
ftz (2)	84B1-2	F1c-d
Antp (1)	84B1-2	F1c-d
DS08506 (2)	84B1-2	F1c-d
α-Est3 (2)	84D8-10	F5e-6a
α-Est10 (2)	84D8-10	F5e-6a
dsx (2)	84E1-2	E1b
Syn (2)	86A4-5	G2b
DS08785 (2)	86D1-2	E4a

(1) Ranz *et al*., 1997; (2) Ranz, 1998.

Quan dos o més marcadors de la mateixa banda o bandes molt properes de *D. melanogaster* han donat un senyal a la mateixa banda de *D. repleta* i *D. buzzatii* s'ha considerat que aquests marcadors formen un segment conservat evolutivament. La mida de les regions i els segments conservats s'ha calculat a l'espècie de referència, *D. melanogaster*, com la distància entre els extrems més llunyans dels marcadors que limiten el segment (Material i Mètodes, apartat 2.2.4.7). El recobriment aconseguit en una regió és el quocient entre la longitud total de la zona coberta per marcadors i la mida de la regió. A la Figura 7 es mostren el resultats obtinguts en les tres regions estudiades.

3.1.3.1. Regió 83E1-84E1

Aquesta regió està limitada pels marcadors DS01673 (83E1-2) i *dsx* (84E1). La mida de la regió és de 1.814 kb. Hi ha en total 21 marcadors amb els quals s'ha aconseguit un recobriment del 74,89%. Els marcadors hibriden en 7 punts independents en els cromosomes de *D. repleta* i *D. buzzatii*, i defineixen 4 segments conservats amb les següents mides: DS01673-DS8128 de 141 kb, DS05926-DS07437 de 166 kb, *Pb*-DS07700 de 335 kb i DS00184-DS05426 de 599 kb (Figura 7). A la Figura 6 es mostra la hibridació d'alguns marcadors d'aquesta regió sobre cromosomes de *D. melanogaster* i de *D. buzzatii* (*2jz*^{3}).

3.1.3.2. Regió 86A4-E2

Aquesta regió està limitada pels marcadors *Syn* (86A4-5) i DS02168 (86E1-2). La mida de la regió és de 1.139 kb. Hi ha un total de 13 marcadors i un recobriment del 81,79%. Els marcadors hibriden en 8 punts independents en els cromosomes de *D. repleta* i *D. buzzatii*, i defineixen 2 segments conservats amb les següents mides: DS05661-DS01137 de 306 kb i DS04597-DS08785 de 320 kb (Figura 7). A la Figura 6 es mostra la hibridació d'alguns marcadors d'aquesta regió sobre cromosomes de *D. melanogaster* i de *D. buzzatii* (*2jz*^{3}).

3.1.3.3. Regió 97B1-E6

La mida d'aquesta regió és de 732 kb i està limitada pels marcadors DS06282 (97B1-3) i 171D2 (97E4-6). Hi ha un total de 25 marcadors i una cobertura del 74,79%. Els marcadors hibriden en 7 punts independents en els cromosomes de *D. repleta* i *D. buzzatii*, i defineixen 4 segments conservats amb les següents mides: DS00612-DS01035 de 86 kb, DS05785-DS02698 de 137 kb, *Rb97D-ro* de 23 kb i 147A8-171D12 de 154 kb (Figura 7). A la Figura 6 es mostra la hibridació d'alguns marcadors d'aquesta regió sobre cromosomes de *D. melanogaster* i de *D. buzzatii* (*2jq*^{7}).

Figura 7. Organització molecular de les regions cromosòmiques 83E1-84E1, 86A4-E2 i 97B1-E6 a *D. repleta*. Els gens es representen com rectangles buits, els cosmidis com rectangles grisos, i els bacteriòfags P1 com rectangles negres.

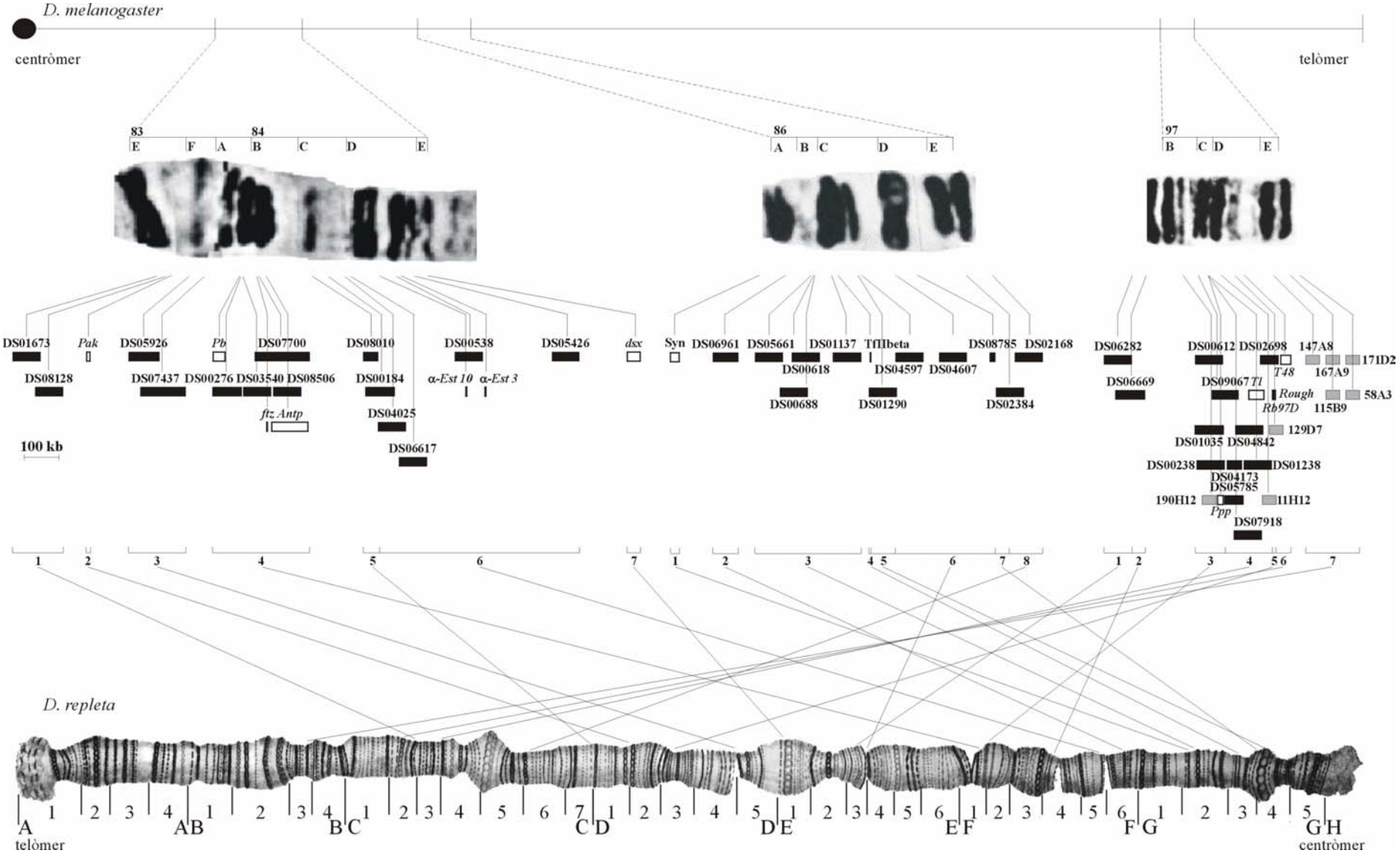
D. melanogaster
centròmer
telòmer
83
E F A
84
B C D E
86
A B C D E
97
B C D E
DS01673
Pak
DS05926
Pb
DS07700
DS08010
DS00538
DS05426
dsx
Syn
DS06961
DS05661
DS01137
TfIIbeta
DS08785
DS02168
DS08128
DS07437
DS00276
DS03540
DS08506
DS00184
α-Est 10
α-Est 3
ftz Antp
DS04025
DS06617
100 kb
DS00618
DS04597
DS04607
DS00688
DS01290
DS02384
DS06282
DS06669
DS00612
DS02698
147A8
171D2
T48
167A9
DS09067
Tl
Rough
58A3
Rb97D
115B9
129D7
DS01035
DS04842
DS00238
DS01238
DS04173
DS05785
190H12
11H12
Ppp
DS07918
D. repleta
A
AB
BC
CD
DE
EF
FG
GH
telòmer
centròmer

3.1.4 Cartografia dels punts de trencament les inversions $2q^7$ i $2z^3$

Els marcadors cartografiats prèviament prop dels punts de trencament de les inversions $2q^7$ i $2z^3$ s'havien hibridat sobre cromosomes de *D. buzzatii* amb l'ordenació estàndard. Per determinar si es trobaven dins o fora de la inversió es van cartografiar sobre cromosomes amb les ordenacions $2jq^7$ i $2jz^3$. L'objectiu era determinar si algun punt de trencament d'aquestes inversions es trobava dins d'un segment conservat. Per això s'han cartografiat marcadors adjacents als marcadors inicials als cromosomes de *D. melanogaster*, sobre soques de *D. buzzatii* portadores de les inversions. Els marcadors de les regions 95A1-96A23 i 97B1-E6 de *D. melanogaster* s'han cartografiat sobre cromosomes $2jq^7$, i els de les regions 83E1-84E1 i 86A4-E2 sobre cromosomes amb l'ordenació $2jz^3$. Els resultats es mostren a les Figures 8 i 9.

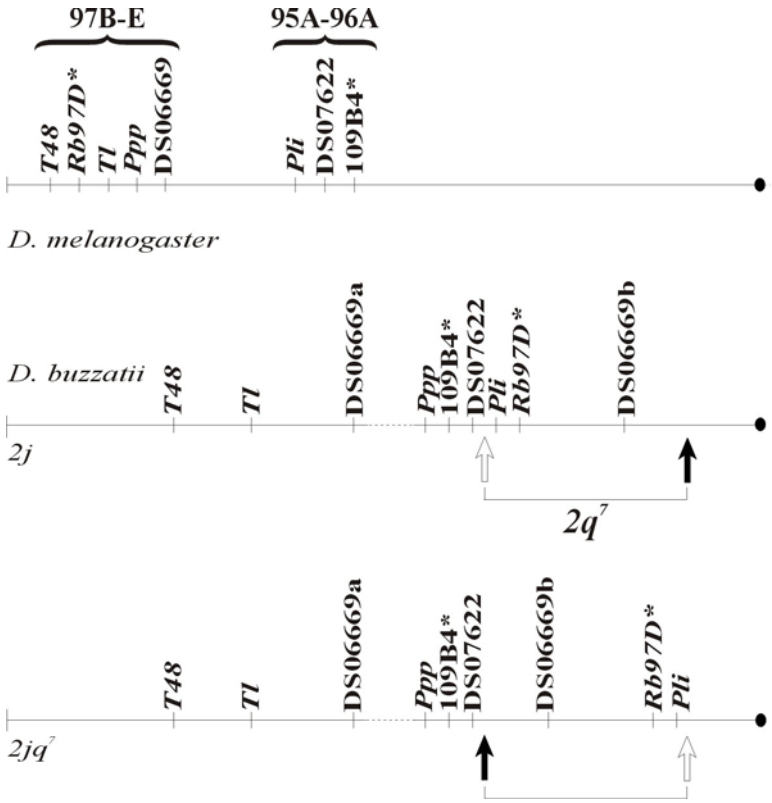

Figura 8. Cartografia dels punts de trencament de la inversió $2q^7$ de *D. buzzatii*. Els marcadors amb asterisc són els cartografiats prèviament. Només es representa un marcador per cada grup de marcadors que hibrida a la mateixa zona a *D. buzzatii*. Quan un marcador produeix dos senyals es diferencien amb les lletres a i b.

En el cas de la inversió $2q^7$ el gen *ro* i el cosmidi 129D7 es van cartografiar dins de la inversió, a la mateixa banda que el marcador inicial (*Rb97D*). Els marcadors que els envolten (els del segment que inclou *Tl* per un costat i *T48* per l'altre) van hibridar a les bandes C4a i C2c respectivament, allunyades del punt de trencament. Casualment els marcadors del següent segment (que inclou *Ppp*) van hibridar a la banda F1h, fora de la inversió i prop del punt de trencament distal. El punt de trencament no pot estar inclòs dins del segment format entre aquests marcadors i *Rb97D* perquè els marcadors intermitjos (el segment de *Tl*) es troben allunyats d'aquesta posició. A més, entre els marcadors del segment de *Ppp* i el punt de trencament s'havien cartografiat ,també fora de la inversió, els marcadors 58B10 i 109B4, procedents de la regió 95A-96A de *D. melanogaster*. L'organització molecular d'aquesta regió a *D. buzzatii* s'havia estudiat per Ranz *et al*. (1999), però les zones que envolten 58B10 i 109B4 no s'havien recobert completament amb marcadors. Els següents marcadors de la regió 95B-C que es van hibridar es van apropar més al punt de trencament (segment que inclou DS07662), fins que DS05188 i *Pli* van hibridar dins de la inversió. Per tant el punt de trencament distal de la inversió $2q^7$ es trobava dins d'un segment conservat. La posició citològica dels marcadors fora de la inversió (D3c-d) i dins de la inversió (D3c) ha permès cartografiar a la banda D3c el punt de trencament distal de la inversió. Prèviament el punt de trencament distal de la inversió s'havia localitzat a la banda D3a (Ruiz *et al*. 1984; Ruiz i Wasserman 1993).

L'únic clon de *D. melanogaster* que cobria l'espai entre els marcadors situats fora i dins de la inversió era el YAC (cromosoma artificial de llevat) DY852 (Cai *et al*. 1994). Aquest clon va hibridar a les bandes D3c-d/D1e/A3f/F5e/C6b-c. El clon va donar un senyal a cada punt de trencament, indicant que conté el punt de trencament distal de la inversió. La resta de senyals coincideixen amb les descrites pels marcadors situats a les bandes que inclou DY852 (Ranz *et al*. 1999). Es va intentar subclonar el clon DY852 per trobar un segment més petit que contingués el punt de trencament. Amb aquest fragment es podria rastrejar una genoteca de *D. buzzatii* i obtenir segments d'aquesta espècie que continguessin el punt de trencament. Els punts de trencament de la inversió *2j* de *D. buzzatii* s'havien clonat seguint un procediment similar (Cáceres *et al*. 1999b). La poca quantitat de DNA del YAC que s'obtenia en les extraccions van fer impossible elaborar un mapa de restricció del clon i per tant obtenir un fragment més petit que contingués el punt de trencament.

Dels dos marcadors situats dins de la inversió (DS05188 i *Pli*), i segons la seva posició a *D. melanogaster*, el gen *Pli* havia d'estar més a prop del punt de trencament que DS05188. Mitjançant un *Southern blotting* amb una sonda de l'extrem 3' de *Pli* sobre diferents digestions de DNA genòmic de les soques j-19 (sense la inversió) i jq^7-4 (amb la inversió) es va veure que la distància màxima entre *Pli* i el punt de trencament era de 6 kb. Aquesta distància és inferior a la mida mitja dels inserts dels bacteriòfags λ utilitzats per construir les genoteques. Per tant, el gen *Pli* es va poder utilitzar per clonar el punt de trencament distal de la inversió (veure resultats, apartat 3.2).

En el cas de la inversió $2z^3$ es va determinar que el gen *Antp* estava dins de la inversió i els gens *α-Est3* i *α-Est10* fora d'ella. Aquests gens provenen de la mateixa regió de *D. melanogaster* que *Antp*, i per tant semblava que els tres gens formaven un segment conservat. Aquest segment inclouria el punt de trencament proximal de la inversió. Per comprovar-ho es van hibridar marcadors situats entre *Antp* i les *α-esterases*. Alguns marcadors van seguir hibridant prop de *Antp* (F1c-d) i les *α-esterases* (F5e-6a), però els marcadors DS00184 i DS08010 van donar un senyal a la banda C7e, allunyada dels punts de trencament de la inversió. Això indica que el segment no està conservat. Els marcadors que limiten amb *Antp* i les *α-esterases* pels altres extrems van seguir hibridant a la mateixa zona fins arribar a DS07437 i *dsx*, que van hibridar a les bandes D5a i E1b respectivament, lluny dels punts de trencament. Per altra banda, els bacteriòfags P1 DS08785, DS04607 i DS04597 havien hibridat a la banda E4a, dins de la inversió i prop del punt de trencament distal. Els marcadors adjacents a *D. melanogaster*, DS01290 i DS02384-DS02168, van hibridar a les bandes G4c i C6a-c respectivament, lluny del punt de trencament. Per tant, no es va trobar cap segment conservat entre *D. melanogaster* i *D. buzzatii* que contingués un punt de trencament de la inversió $2z^3$. Els punts de trencament de la inversió s'havien localitzat a les bandes C6c i F1c (Ruiz *et al*. 1984; Ruiz i Wasserman 1993). Posteriorment, i basant-se en la localització d'un marcador prop del punt de trencament proximal de la inversió i en observacions de la morfologia dels cromosomes, es va proposar que el punt de trencament distal de la inversió es localitzava a la banda E4b-c (Laayouni *et al*. 2000). La posició de *pb* (F1e) i DS00276 (F1c-e), que es mantenen dins de la inversió, fa que el punt de trencament proximal no pugui estar localitzat a la banda F1c. Segons la posició d'aquests marcadors i les observacions de cromosomes portadors i no portadors

de la inversió, el punt de trencament proximal es troba a la banda F1f. La posició del punt de trencament distal coincideix, segons aquestes observacions, amb la proposada per Laayouni *et al*. (2001), a la banda E4b-c.

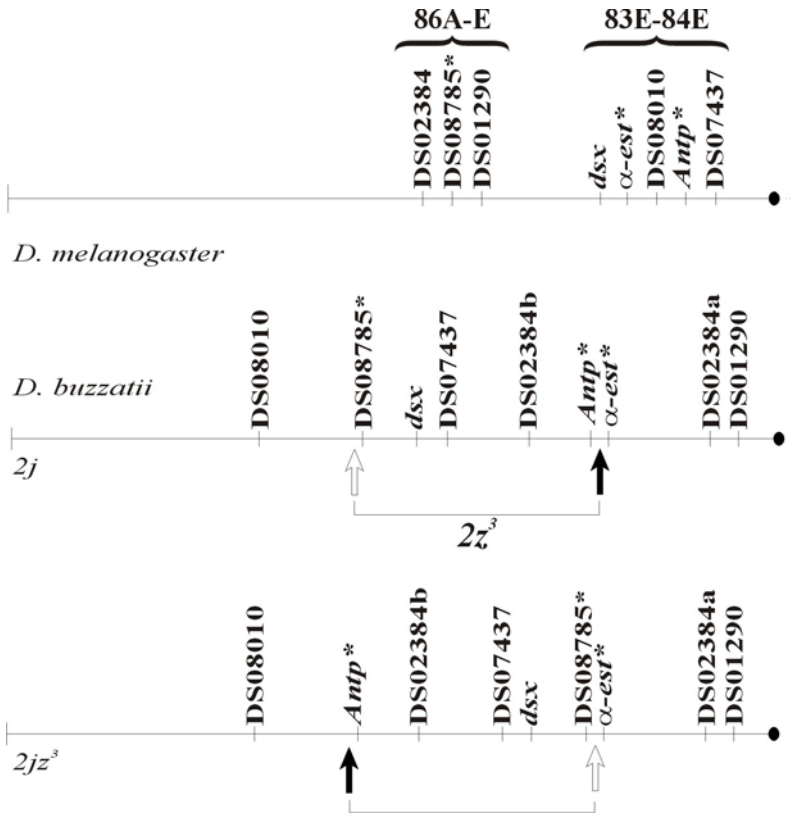

Figura 9. Cartografia dels punts de trencament de la inversió $2z^3$ de *D. buzzatii*. Els marcadors amb asterisc són els cartografiats prèviament. Només es representa un marcador per cada grup de marcadors que hibrida a la mateixa zona a *D. buzzatii*. Quan un marcador produeix dos senyals es diferencien amb les lletres a i b.

3.1.4.1 Localització de sondes de la regió 21A-C de *D. virilis* a *D. buzzatii*

Un dels marcadors cartografiats prop del punt de trencament distal de la inversió $2q^7$, el gen *ro*, està cartografiat a la banda 21A6-7 de *D. virilis*. Aquest gen està situat en un segment de *D. buzzatii* limitat per *ro* i els cosmidis 58B10 i 109B4 que conté el punt de trencament distal de la inversió $2q^7$. Davant de la possibilitat de disposar de clons d'una genoteca de bacteriòfags P1 de *D. virilis* (Lozovskaya *et al*. 1993; Vieira *et al*. 1997) es va comprovar si aquest segment estava conservat a aquesta espècie. Per fer-ho es van hibridar els clons DS07442 (fora de la inversió) i DS05188 (dins de la inversió)

sobre cromosomes de *D. virilis*. Els marcadors es van cartografiar prop de *ro* (Taula 11), i per tant es van hibridar tots els clons disponibles de la mateixa regió.

Taula 11. Resultat de les hibridacions de sondes de la regió 21A-21C de *D. virilis*.

Sonda	***D. virilis***		***D. buzzatii***
	Literatura	**Aquest treball**	
Dv11-23 [c]	21A	21A1-2	F5d-e
Dv11-67 [c]	21A	21A1-2	F5d-e
Dv11-68 [c]	21A	21A1-2	F5d-e
Dv11-85 [c]	21A	21A3-5	F5d-e
Dv12-74 [c]	21A	21A4-5	F6a
DS07442 [c]	ND	21A6	D3c-d
DS05188 [c]	ND	21A7	D3c
ro [a]	21A6-7	21A7	D3b-c
Dv1-30 [c]	21A	21B1-2	D3b
Dv14-24 [c]	21B	21B2	D2g
Dv68-94 [c]	21B	21B2	D2g
Dv71-12 [c]	21B	21B2	D2g
Dv71-72 [c]	21B	21B2-3	D2f-g
Dv71-65 [c]	21B	21B2-3	D2f
Dv71-16 [c]	21C	21B2	D2g

[a] sondes gèniques; [c] bacteriòfags P1.
ND, no determinat.

Aquests clons es van hibridar sobre cromosomes de *D. virilis* (hibridacions control) i sobre cromosomes de *D. buzzatii* amb la inversió *2q*[7], per veure si algun contenia el punt de trencament. Els resultats es mostren a la Taula 11. El marcador Dv1-30 es va cartografiar prop del punt de trencament distal de la inversió. El marcador estava situat dins de la inversió i lleugerament més allunyat del punt de trencament que *ro*. La resta de marcadors situats en direcció 21B-C a *D. virilis* es van localitzar a les bandes D2f-g, més allunyades que *ro* del punt trencament. La resta de marcadors situats

en direcció 21A van donar senyals a les bandes F5d-F6a, allunyades dels punts de trencament de la inversió.

3. RESULTATS

3.2 Clonació i seqüenciació dels punts de trencament de la inversió *2q*^{7} de *D. buzzatii*

A partir d'un marcador (el gen *Pli*) cartografiat prop del punt de trencament distal de la inversió *2q*^{7} de *D. buzzatii* es van clonar els punts de trencament d'aquesta inversió. L'anàlisi de les seqüències dels punts de trencament va revelar la presència d'insercions d'elements transposables a totes les soques portadores de la inversió. La organització de les seqüències que limiten amb els elements transposables mostren que probablement *Galileo*, un element de tipus *Foldback*, va originar la inversió. L'anàlisi de la seva seqüència suggereix que la inversió es va originar per recombinació ectòpica entre dues còpies de l'element. La presència d'altres elements transposables i les diferències estructurals que existeixen entre les insercions de diferents soques indiquen que els punts de trencament de la inversió són regions genèticament inestables i punts calents per a insercions d'elements transposables.

Aquests resultats s'han publicat a la revista Molecular Biology and Evolution (volum 20, pàgines: 674-685) amb el títol:

The *Foldback*-like transposon *Galileo* is involved in the generation of two different natural cromosomal inversions of *Drosophila buzzatii*
Ferran Casals, Mario Cáceres i Alfredo Ruiz.

The *Foldback*-like Transposon *Galileo* Is Involved in the Generation of Two Different Natural Chromosomal Inversions of *Drosophila buzzatii*

Ferran Casals, Mario Cáceres,[1] *and Alfredo Ruiz*

Departament de Genètica i de Microbiologia, Universitat Autònoma de Barcelona, Bellaterra (Barcelona), Spain

Chromosomal inversions are the most common type of genome rearrangement in the genus Drosophila. Although the potential of transposable elements (TEs) for generating inversions has been repeatedly demonstrated in the laboratory, little is known on their role in the generation of natural inversions, which are those effectively contributing to the adaptation and/or evolution of species. We have cloned and sequenced the two breakpoints of the polymorphic inversion $2q^7$ of *D. buzzatii*. The sequence analysis of the breakpoint regions revealed the presence in the inverted chromosomes of large insertions, formed by complex assemblies of transposons, that are absent from the chromosomes without the inversion. Among the transposons inserted, the *Foldback*-like element *Galileo,* that was previously found responsible of the generation of the widespread inversion *2j* of *D. buzzatii*, is present at both $2q^7$ breakpoints and is the most likely inducer of the inversion. A detailed study of the nucleotide and structural variation in the breakpoint regions of six chromosomal lines with the $2q^7$ inversion detected no nucleotide differences between them, which suggests a monophyletic and recent origin. In contrast, a remarkable degree of structural variation was observed in the same six chromosomal lines. It thus appears that the two breakpoints of the inverted chromosomes have become genetically unstable hotspots, as was previously found for the *2j* inversion breakpoints. The possibility that this instability is caused by structural properties of *Foldback* elements is discussed.

Introduction

Since the discovery of transposable elements (TEs) in maize, their evolutionary potential for rearranging genomes has been repeatedly emphasized (Finnegan 1989; McDonald 1993). In the laboratory, both class I elements (RNA transposable elements) and class II elements (DNA transposable elements or transposons) have been shown to mediate the generation of deletions, duplications, inversions, and reciprocal translocations (Berg and Howe 1989), and several molecular mechanisms may be involved. The simplest manner in which TEs can induce rearrangements is by acting as substrates for ectopic recombination between homologous TE copies located in different sites of the genome (Petes and Hill 1988; Lim and Simmons 1994). However, several other more complex models, most of them involving aberrant transposition events of transposons, have been put forth and supported empirically (Gray 2000). In recent years a growing body of evidence has shown that TEs are implicated in the origin of natural chromosomal rearrangements in a wide range of organisms, including bacteria (Daveran-Mingot et al. 1998), yeasts (Kim et al. 1998), flies (Cáceres et al. 1999), and hominids (Schwartz et al. 1998).

Perhaps the most extraordinary and intensely studied case of chromosomal variation in eukaryotes is found in the Drosophila genus (Sperlich and Pfriem 1986; Krimbas and Powell 1992). More than half of the Drosophila species are polymorphic for paracentric inversions (Powell 1997), and interspecific comparisons of physical maps reveal an extreme rate of chromosomal rearrangement, with nearly four inversions fixed per lineage and Myr (Segarra et al. 1995; Ranz, Casals, and Ruiz 2001; González, Ranz, and Ruiz 2002). Studies in Drosophila were among the first to show the capacity of TEs to induce chromosomal rearrangements in the laboratory. The implicated TEs include the class I elements *BEL*, *roo*, *Doc*, and *I*, and the class II elements *P, hobo*, and *FB* (Lim and Simmons 1994). In contrast, relatively little is yet known about the origin of natural inversions—i.e., those effectively contributing to adaptation and/or evolution of Drosophila species—and their consequences at the molecular level.

Circumstantial evidence for the implication of TEs in the origin of Drosophila natural inversions was first gathered by in situ hybridization with probes of different TEs in *D. melanogaster* (Lyttle and Haymer 1992), *D. willistoni* (Regner et al. 1996), and the *virilis* species group (Zelentsova et al. 1999; Evgen'ev et al. 2000). However, the molecular characterization of inversion breakpoints yielded diverse or contradictory results. Initially, no traces of TEs were found in the breakpoints of the first two natural inversions characterized at the molecular level: the polymorphic inversion *In(3L)Payne* of *D. melanogaster* (Wesley and Eanes 1994) and an inversion fixed between *D. melanogaster* and *D. suboscura* (Cirera et al. 1995). Later, a new repetitive sequence (designated *Odysseus*) was detected at the distal breakpoint junction of inversion *2Rd′* in the mosquito *Anopheles arabiensis* (Mathiopoulos et al. 1998), and a *LINE*-like retrotransposon was found near one of the breakpoints of inversion *In(2L)t* of *D. melanogaster* (Andolfatto, Wall, and Kreitman 1999). Finally, the clearest evidence to date of the role of TEs in the generation of Drosophila inversions was provided by the *D. buzzatii* widespread *2j* inversion (Cáceres et al. 1999). In this case, both breakpoints contained large insertions made up of the *Foldback*-like element *Galileo* plus several other transposons, which have integrated within or near the original *Galileo* elements (Cáceres, Puig, and Ruiz 2001). The arrangement of target site duplications flanking the *Galileo* copies at each breakpoint strongly suggested that the inversion was generated by ectopic recombination between them (Cáceres et al. 1999). Furthermore, the low nucleotide variability in the

[1] Present address: Laboratory of Genetics, The Salk Institute for Biological Studies, La Jolla, California.

Key words: genome evolution, chromosomal inversions, inversion breakpoints, transposable elements, hotspots, *Drosophila buzzatii*.

E-mail: alfredo.ruiz@uab.es.

Mol. Biol. Evol. 20(5):674–685. 2003
DOI: 10.1093/molbev/msg070

Table 1
Sequence of Oligonucleotide Primers Used for PCR Amplification

Name	Sequence (5′–3′)	Primer Pair
Pli1	CAGCATTCAATCTCGTAC	Pli2
Pli2	TGAGGTATCTCCACATTG	Pli1
A1	GTGAATAACTCGTGCGTGTAA	B1, C1, T1, T2
B1	TTGCGGACGCGATAATGTTAA	A1, D1, T4, T5, T7
C1	GAGGAAACACTCATTGTCTCA	A1, D1, T3
D1	GTATGAAGTGACTGGTGATCA	B1, C1, T3, T6, T8, T9
T1	GCAGCAGCTTACCTGATATG	A1
T2	TTCCAGTTGTCCAGTCTATGT	A1
T3	TTGTTCCAGTTGTCCAGTCTA	C1, D1
T4	GTGTTACTCAATCGTGTGTTG	B1
T5	CGAGCAAATACGAAGATGACT	B1
T6	TGTTCGAGTTGTCCAGTCTAT	D1
T7	GATATAGCGCTTATGGAGTAC	B1
T8	CTTATCCACGAATCATTTTCAG	D1
T9	AACGAGTGATGTGTCAAACTG	D1

breakpoint regions and the clustering of all *2j* chromosomes in a single clade were consistent with the uniqueness of the recombination event and a monofiletic origin of the *2j* inversion (Cáceres et al. 1999; Cáceres, Puig, and Ruiz 2001).

To test how common are these observations and provide further information on the origin of Drosophila natural inversions, we have cloned and sequenced the two breakpoints of another polymorphic inversion of *D. buzzatii*, $2q^7$. The isolation of the breakpoints of this inversion was made possible by the availability of several *D. melanogaster* markers that mapped by in situ hybridization close to its distal breakpoint (Ranz, Casals, and Ruiz 2001). The $2q^7$ inversion differs from the *2j* inversion by three characteristics: (1) The *2j* inversion is located in a middle position of chromosome 2. Inversion $2q^7$ overlaps with inversion *2j* and is located more proximally, with one breakpoint near the centromere (Ruiz and Wasserman 1993);(2) inversion $2q^7$ arose on a *2j* chromosome, giving rise to the $2jq^7$ arrangement, and is more recent than inversion *2j*;(3) inversion *2j* has a widespread distribution and is present at high frequencies in most *D. buzzatii* populations, whereas the $2jq^7$ arrangement has a much restricted geographical distribution and is usually present at rather low frequencies (<10%) (Hasson et al. 1995). Here we show that, despite these differences, the molecular structure of the breakpoint regions is strikingly similar in both inversions. As in the case of inversion *2j*, the $2q^7$ inversion breakpoints contain large insertions made up of *Galileo* plus several other TEs, and they qualify as genetically unstable hotspots (Cáceres, Puig, and Ruiz 2001).

Materials and Methods

Drosophila Stocks

Twenty-seven lines of *D. buzzatii*, one line of *D. koepferae* (KO-2, from Sierra San Luis, Argentina), one line of *D. melanogaster* (Canton S, 1611.2 from The National Drosophila Species Resource Center, Bowling Green, Ohio), and one of *D. virilis* (VIR-Tokyo, Japan) were used. The *D. buzzatii* lines are homokaryotipic for one of four different chromosome 2 arrangements: *2st, 2j,* $2jz^3$, and $2jq^7$. They were isolated from different natural populations covering most of the distribution range of the species and their geographical origin is as follows: st-1, j-1, jz^3-1 and jq^7-1, Carboneras (Spain); st-3, Vipos (Argentina); st-4 and j-12, Guaritas (Brazil); st-5, Catamarca (Argentina); st-6 and j-16, Salta (Argentina); st-7, Termas de Rio Hondo (Argentina); st-8 and j-19, Ticucho (Argentina); st-9, j-22 and jz^3-5, Trinkey (Australia); j-8, San Luis (Argentina); j-9, Quilmes (Argentina); j-10, Palo Labrado (Argentina); j-11, Los Negros (Bolivia); j-17 and jz^3-4, Tilcara (Argentina); jq^7-2, Mogan, Canary Islands (Spain); jq^7-3, Caldetas (Spain); and jq^7-4, jq^7-5 and jq^7-6, Otamendi (Argentina).

Probes and in Situ Hybridization

Three gene clones (*Pli, Rb97D*, and *ro*), two cosmid clones, and six P1 phages were used as probes for in situ hybridization to map the distal breakpoint of the $2q^7$ inversion. The *Pli* clone contains 1.6 kb from the 3′ end of the *Pli* (*Pellino*) gene (Grosshans, Schnorrer, and Nusslein-Volhard 1999) and was obtained by polymerase chain reaction (PCR) amplification of *D. melanogaster* genomic DNA with appropriate primers (table 1) and cloning of the PCR product into the pGEM-T vector (Promega). All remaining clones come from *D. melanogaster*, except that containing the *ro* gene that comes from *D. virilis*, and were kindly provided by different authors (*Rb97D* and *ro*; see Ranz, Casals, and Ruiz 2001), the European Drosophila Genome Project (cosmids), or the Berkeley Drosophila Genome Project (P1 phages). In situ hybridization of DNA probes to the larval salivary gland chromosomes was carried out using the procedure described by Montgomery, Charlesworth, and Langley (1987). All probes were labeled with biotin-16-dUTP (Roche) by nick translation, and detection was carried out with the ABC-Elite Vector Laboratories kit. The *D. melanogaster* clones were hybridized to the chromosomes of *D. melanogaster* (Canton S) as control and to the chromosomes of a *2j* line (j-1) and a $2jq^7$ line (jq^7-4) of *D. buzzatii* for breakpoint mapping. The *ro* probe was hybridized to the chromosomes of *D. virilis* as control, as well as to the chromosomes of *D. melanogaster* and *D. buzzatii*. In addition, during the isolation of the breakpoint regions (fig. 1) λ phages derived from *D. buzzatii* genomic libraries and their subclones were hybridized to the chromosomes of the j-1 and jq^7-4 lines. Heterologous (interspecific) hybridizations were performed at 25°C, and homologous (intraspecific) hybridizations were completed at 37°C. Cytological localization of the hybridization signals was determined from the cytological maps of *D. buzzatii* (Ruiz and Wasserman 1993) and the photographic and electron microscopy maps of *D. melanogaster* (Lefevre 1976; Heino, Saura, and Sorsa 1994).

Construction and Screening of Genomic Libraries

A genomic library was constructed with DNA derived from the jq^7-4 line of *D. buzzatii* using the

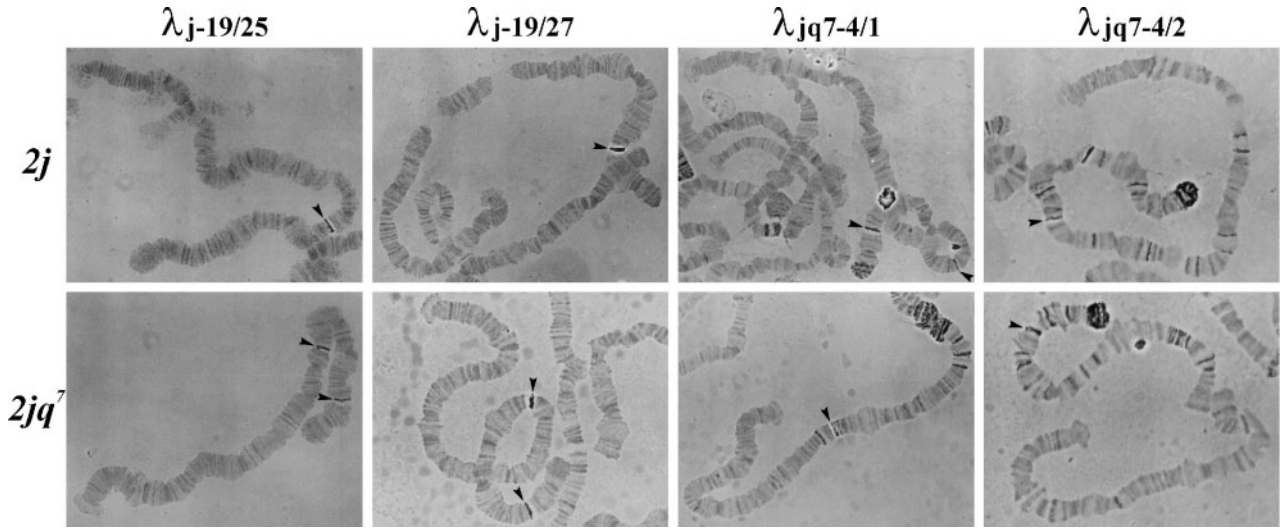

FIG. 1.—In situ hybridization of lambda clones λj-19/25, λj-19/27, λjq7-4/1, and λjq7-4/2 to the salivary gland chromosomes of *D. buzzatii* lines j-19 (*2j* arrangement) and jq^7-4 (*2jq*^{7} arrangement). Arrows indicate hybridization signals corresponding to the *2q*^{7} inversion breakpoint regions. Clones λj-19/25 and λj-19/27 produce a single hybridization signal on the *2j* arrangement but two signals on the *2jq*^{7} chromosomes, and contain the distal (AB) and proximal (CD) breakpoint regions, respectively. Clone λjq7-4/1 produces a strong signal on the *2jq*^{7} arrangement and two signals on the *2j* arrangement and encompasses the distal breakpoint region (AC). Clone λjq7-4/2 hybridizes strongly to the proximal breakpoint region in the *2jq*^{7} arrangement and to the distal breakpoint on the *2j* arrangement, and seems to contain at least part of the proximal breakpoint region (BD). The last two clones, λjq7-4/1 and λjq7-4/2, show additional hybridization signals at other chromosomal sites (including the centromere) owing to the presence of repetitive DNA.

LambdaGEM-11 vector according to the manufacturer's instructions (Promega). Briefly, high molecular weight genomic DNA was randomly fragmented by partial digestion with *Sau* 3A, electrophoresed on a 0.4% agarose gel, and fragments of 15–23 kb were recovered and ligated with the lambda vector arms. This library and a lambda genomic library of the j-19 line (Cáceres, Puig, and Ruiz 2001) were screened by plaque hybridization with the probes indicated in text. The j-19 library was previously amplified following the procedures described in Sambrook, Fritsch, and Maniatis (1989). DNA fragments of interest from positives phages were subcloned into Bluescript II SK vector (Stratagene) after restriction enzyme digestion and gel purification.

Southern Analysis

Southern hybridization was carried out according to standard procedures (Sambrook, Fritsch, and Maniatis 1989). Probes were labeled by random primer with digoxygenin-11-dUTP under the conditions specified by the supplier (Roche). The probes used were *Pli* (the Pli1-Pli2 *D. melanogaster* PCR product of 1.6 kb), AB (the A1-B1 *D. buzzatii* PCR product of 0.6 kb), and CD (the *Cla* I *D. buzzatii* restriction fragment of 0.9 kb; see below). Hybridization was carried out overnight in standard buffer with 50% formamide at 42°C for homologous probes (AB and CD) and at 37°C for heterologous probes (*Pli*). Stringency washes were performed with 0.1 × SSC 0.1% SDS solution at 68°C and 50°C for homologous and heterologous hybridizations, respectively.

PCR Amplification

Polymerase chain reaction testing was carried out in a volume of 50 μl, including 100–200 ng of genomic DNA, 20 pmols of each primer, 200 μM dNTPs, 1.5 mM $MgCl_2$, and 1–1.5 units of Taq DNA polymerase. Temperature cycling conditions were 30 rounds of 30 s at 94°C; 30 s at the annealing temperature, and 60 s at 72°C, with annealing temperature varying from 58° to 68°C depending on the primer pair used. Amplifications of the A1-B1 and C1-D1 fragments in *D. koepferae* were performed at 54°C. Sequences of oligonucleotide primers are given in table 1. Two primer pairs (A1-B1 and C1-D1) were used to amplify the inversion breakpoint regions (AB and CD) in *D. buzzatii* lines without the inversion (*2st, 2j*, and *2jz*^{3}) and *D. koepferae*. Different primer combinations (see table 1) were tested to amplify the inversion breakpoint regions (AC and BD) of lines with the *2q*^{7} inversion (*2jq*^{7}).

DNA Sequencing and Sequence Analysis

Sequences were obtained on an ABI 373 A (Perkin-Elmer) automated DNA sequencer. Fragments cloned into Bluescript II SK or pGEM-T were sequenced with M13 universal and reverse primers. The PCR products were gel-purified using the Geneclean Spin Kit (Bio 101) and sequenced directly with the same primers used for amplification. To estimate the nucleotide variation of the distal and proximal breakpoints region, the A1-B1 and C1-D1 PCR products were sequenced in a sample of nine *2st*, *2j*, or *2jz*^{3} lines without the inversion. In addition, PCR products obtained with primer pairs A1-T1, B1-T4 (B1-T5 in line jq^7-6), T3-C1, and T9-D1 were sequenced in all *2jq*^{7} lines to determine the exact location of the insertions present in the inversion breakpoints and to estimate the nucleotide diversity. Nucleotide sequences were analyzed with the Wisconsin Package (Genetics Computer Group). BESTFIT was used to compare homologous sequences in

Table 2
Markers from *D. melanogaster* Hybridized to the Chromosomes of *D. buzzatii* for the High-Resolution Mapping of the $2q^7$ Inversion Distal Breakpoint and Their Position in Relation to the Inversion

	Chromosomal Site		
Marker	*D. melanogaster*	*D. buzzatii*	Relation to the $2q^7$ Inversion
109B4	95B7-9	D3d	Outside
58B10	95B7-9	D3d	Outside
DS05515	95B7-9	D3c-d	Outside
DS07442	95C1-4	D3c-d	Outside
DS00619	95C1-7/multiple signals	D3c-d	Outside
DS04424	95C1-7/multiple signals	D3c-d	Outside
DS07662	95C1-7/multiple signals	D3c-d	Outside
Pli	95C7-C9	D3c	Inside
DS05188	95C7-C11	D3c	Inside
Ro	97D5	D3b-c	Inside
Rb97D	97D5	D3b-c	Inside

different lines and to detect changes between them. Similarity searches in the GenBank/EMBL databases were carried out using BLASTX, TBLASTX, and FASTA. Nucleotide variation between the different *D. buzzatii* strains was obtained by multiple alignments of the sequences with ClustalW (Thompson, Higgins, and Gibson 1994), followed by analysis with the DnaSP version 3.51 software (Rozas and Rozas 1999).

Results

High-Resolution Mapping of the $2q^7$ Inversion Distal Breakpoint

Cytological studies localized the distal and proximal breakpoints of inversion $2q^7$ near bands D3a and G2f, respectively, of chromosome 2 of *D. buzzatii* (Ruiz and Wasserman 1993). Our detailed physical map of chromosome 2 in *D. buzzatii* and *D. repleta* (Ranz, Casals, and Ruiz 2001) allowed us to find two cosmids 109B4 and 58B10, which mapped in band D3d of *D. buzzatii* chromosome 2, outside inversion $2q^7$ and not far from its distal breakpoint (table 2). Seven additional available markers (one gene clone and six P1 phages) from the 95B-C region of *D. melanogaster* were therefore hybridized to $2jq^7$ chromosomes of *D. buzzatii* (table 2). All mapped very close to the distal breakpoint of inversion $2q^7$. Two of them, the gene *Pli* and the P1 phage DS05188, were located inside the inversion, whereas the remaining five P1 phages were located outside the inversion (table 2). The cytological position of these markers points to band D3c of *D. buzzatii* chromosome 2 as the precise site of the $2q^7$ distal breakpoint. To estimate the distance from *Pli* to the $2q^7$ distal breakpoint in *D. buzzatii*, we carried out a Southern hybridization of genomic DNA from *2j* and $2jq^7$ chromosomal lines digested with the restriction enzymes *Bam* HI, *Hind* III, *Pst* I, and *Sal* I with a 1.6 kb *Pli* probe. In *Bam* HI, *Pst* I, and *Sal* I digestions, hybridization bands differed between the lines with and without the $2q^7$ inversion, indicating that *Pli* was very close to the breakpoint. Specifically, we located *Pli* and the distal breakpoint within a *Sal* I fragment of 6 kb in the *2j* chromosome.

Isolation and Sequencing of the $2q^7$ Inversion Breakpoints

According to previous studies (Wesley and Eanes 1994; Cáceres et al. 1999), the distal and proximal breakpoint regions were designated as AB and CD in the non-inverted chromosomes (*2st*, *2j*, or $2jz^3$) and as AC and BD in the inverted chromosomes ($2jq^7$) (fig. 2). To isolate the distal breakpoint of inversion $2q^7$ in the non-inverted arrangement, ~75,000 phages of a lambda genomic library derived from a *2j* line (j-19; Cáceres, Puig and Ruiz 2001) were screened with the *Pli* probe, and four positive clones were obtained. These four clones mapped by in situ hybridization to band D3c of *2j* chromosomes and produced two hybridization signals at both $2q^7$ inversion breakpoints in $2jq^7$ chromosomes, indicating that they spanned the distal breakpoint region (AB). Figure 1 shows the hybridization pattern of one of the four clones, λj-19/25. A restriction map of this clone was made and several subclones were hybridized to chromosomes with and without the $2q^7$ inversion, locating the distal breakpoint first in a 6 kb *Sal* I-*Sau* 3A fragment (pGPE205) and then in a 1.9 kb *Bam* HI-*Hind* III fragment (pGPE205.1). The latter fragment and the adjacent 1 kb *Hind* III fragment (pGPE205.3) were completely sequenced (fig. 2).

To clone the proximal (AC) and distal (BD) breakpoints in the chromosome with the inversion, a lambda genomic library was constructed from a $2jq^7$ chromosomal line (jq^7-4), and ~60,000 phages were screened with the AB subclone (pGPE205.1). Twenty-one positive phages were obtained. These phages were rescreened independently with A and B probes, and two phages—λjq7-4/1 and λjq7-4/2—that hybridized with pGPE205.2 and pGPE205.3, respectively, were selected (fig. 2). In situ hybridization of λjq7-4/1 produced an intense signal at the distal breakpoint on $2jq^7$ chromosomes but two signals at both breakpoints of *2j* chromosomes (fig. 1), corroborating that it spanned the distal breakpoint region (AC). Likewise, hybridization of clone λjq7-4/2 produced intense signals at the proximal breakpoint (BD) on $2jq^7$ chromosomes and the distal breakpoint (AB) on *2j* chromosomes (fig. 1), indicating that the clone came from the proximal breakpoint region. It is worthwhile to note, however, that both λjq7-4/1 and λjq7-4/2 phages produced additional weaker signals at different euchromatic sites and stained heavily the centromeres of all chromosomes (fig. 1), which suggests that both of them contain repetitive sequences.

By Southern hybridization with the pGPE205.1 probe, the sequences of λjq7-4/1 homologous to the A region were identified in a 2 kb *Bam* HI-*Hind* III fragment (pGPE209), and the sequences of λjq7-4/2 homologous to the B region were found in a 6-kb *Hind* III fragment (pGPE208) (fig. 2). These two fragments were subcloned and completely sequenced. In addition to sequences homologous to the single-copy A and B sequences found in non-inverted chromosomes, they contained sequences homologous to TEs already described in *D. buzzatii* (Cáceres, Puig, and Ruiz 2001). To complete the isolation of the distal breakpoint region (AC), three fragments contiguous with pGPE209 were cloned and sequenced:

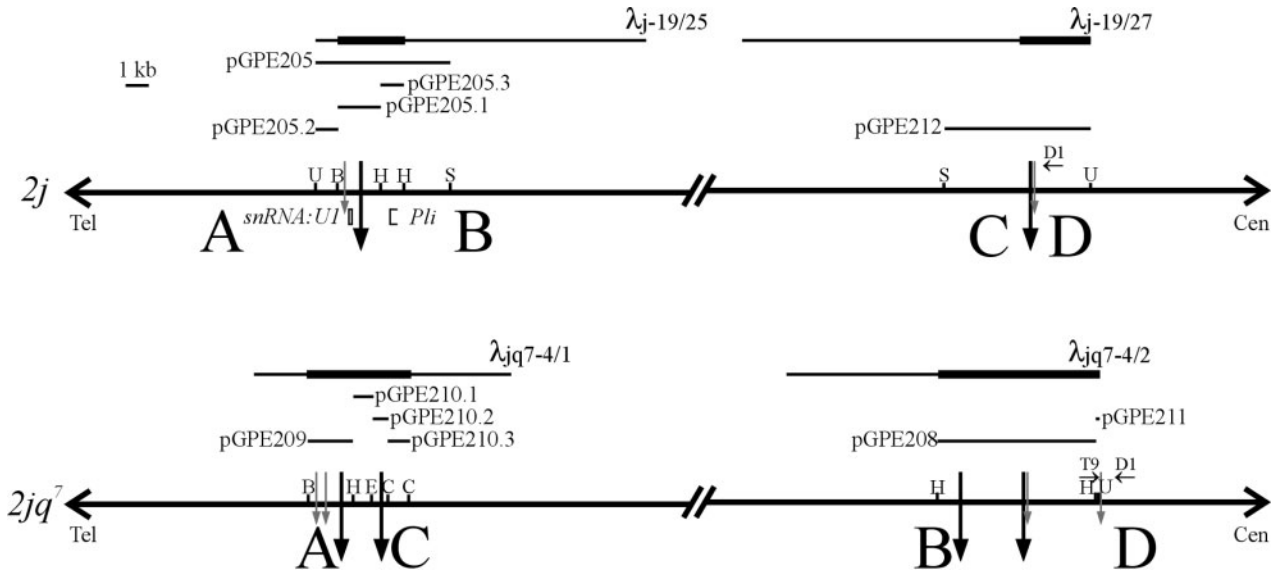

FIG. 2.—Experimental strategy for cloning the breakpoint regions of the $2q^7$ inversion. The breakpoint regions are designated AB and CD in the non-inverted chromosome (*2j*) and AC and BD in the inverted chromosome ($2jq^7$). Lines above the map represent the lambda clones isolated during the cloning of the $2q^7$ breakpoints and some of the subclones derived from them. Thick segments of the lambda clones represent sequenced regions (sequence analysis is shown in fig. 3). Horizontal arrows represent the primers employed to complete the isolation of the BD region in the inverted chromosome. Long vertical arrows mark the location of the breakpoints and the limits of the insertions found at the breakpoints in the inverted chromosomes. Short vertical arrows limit other insertions found in the inverted chromosome and show its corresponding location in the non-inverted chromosome. Empty boxes represent genes sequenced totally (*snRNA:U1*) or partially (*Pli*). Cen: centromere; Tel: telomere. Restriction sites: B: *Bam* HI; C: *Cla* I; E: *Eco* RI; H: *Hind* III; S: *Sal* I; U: *Sau* 3A.

a 0.9 kb *Hind* III-*Eco* RI band (pGPE210.1), a 0.7 kb *Eco* RI-*Cla* I band (pGPE210.2), and a 1 kb *Cla* I band (pGPE210.3) (fig. 2). Sequence analysis revealed the presence of repetitive DNA in pGPE210.1 and pGPE210.2, and sequences homologous to *D. melanogaster* single-copy DNA, presumably from the C region, in pGPE210.2 and pGPE210.3. In the proximal breakpoint region (BD), the sequencing of the outermost 90 bp *Hind* III-*Sau* 3A fragment of λjq7-4/2 (pGPE211) (fig. 2) revealed that it contained only repetitive sequences similar to those in pGPE208. Thus, the D region in the inverted chromosome ($2jq^7$) was obtained after the cloning and sequencing of the proximal breakpoint region (CD) in the non-inverted chromosome (*2j*) (see below) by PCR amplification with primers T9 and D1 (fig. 2). Sequencing of the PCR product of 671 bp showed that it contained repetitive sequences and single-copy DNA from D.

Finally, the proximal breakpoint region (CD) in the chromosome without the inversion (*2j*) was isolated by screening the j-19 lambda genomic library with pGPE210.3 (fig. 2). Five positive phages were obtained, and all of them were shown by in situ hybridization to span the CD breakpoint (fig. 1). A restriction map of one of them, λj-19/27, was made and the breakpoint was further located to a 6.5 kb *Sal* I-*Sau* 3A fragment (pGPE212) by in situ hybridization of different λj-19/27 subclones. This clone was partially sequenced, and 3.1 kb of single-copy sequence from the CD region were obtained.

Sequence Analysis of the Breakpoint Regions

Overall, we sequenced 2,933 bp and 3,095 bp of the AB and CD $2q^7$ breakpoint regions, respectively, in a *2j* line (j-19), and 4,565 bp and 6,751 bp of the AC and BD $2q^7$ breakpoint regions in a $2jq^7$ line (jq^7-4). Comparison of the breakpoint sequences in the non-inverted (AB and CD) and inverted (AC and BD) chromosomes allowed us to determine the exact boundaries of the inverted segment and to identify the repetitive sequences inserted at the breakpoint junctions (fig. 3).

In the line without the inversion (j-19), the genes *snRNA:U1* and *Pellino* (*Pli*) were found flanking the distal breakpoint (AB), with the *Lsp-1*β gene located also in the A region further away from the breakpoint. The proximal breakpoint (CD) was flanked by the *CG1172* gene and by a *tRNA-thr* gene (fig. 3). This same A, B, C, and D single-copy sequences were present in the line with the inversion (jq^7-4), but in an AC and BD arrangement, with B and C sequences in the inverted orientation (fig. 3). In addition, some small deletions were detected with respect to the j-19 chromosome, consisting of 23 nucleotides precisely located at the A-B junction and 45-bp located 89 bp away from the breakpoint in A. More importantly, several large insertions were found in the AC and BD breakpoint regions of the $2jq^7$ chromosome (fig. 3). In the distal breakpoint there is a 1.8-kb insertion just in the A-C juncture and a 387-bp insertion in the A region, between the *Lsp-1*β and *snRNA:U1* genes (fig. 3). In the proximal breakpoint region (BD) there are two insertions of 2.4 and 3 kb separated by 11 bp only (CTTGTTCCCAG), which corresponds to the first 11 nucleotides of the D sequence (fig. 3).

The sequences of all these large insertions showed high identity with a set of TEs previously found in *D. buzzatii* (Cáceres, Puig, and Ruiz 2001). The only exception is the 387-bp insertion in A that shows all the

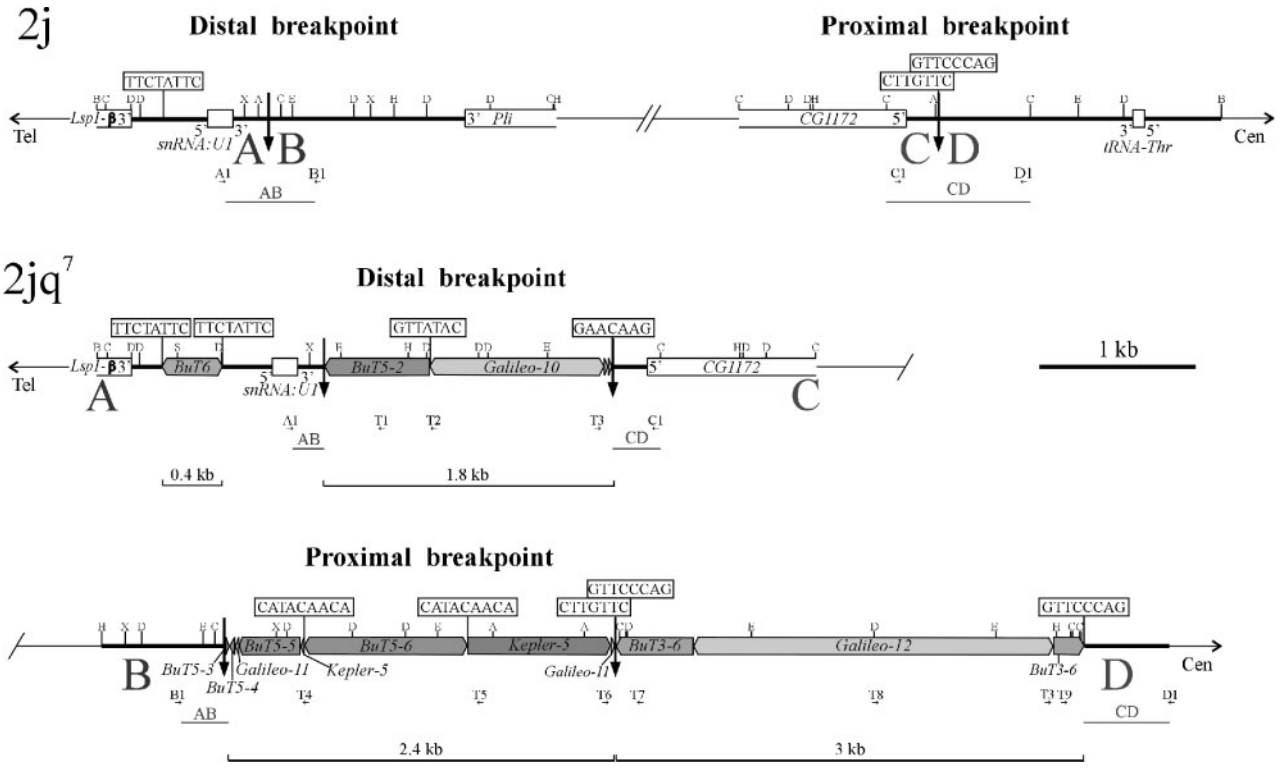

FIG. 3.—Schematic diagram of the sequenced regions of the $2q^7$ inversion breakpoints in *D. buzzatii* lines j-19 (*2j* arrangement) and jq^7-4 ($2jq^7$ arrangement). Thick lines represent the single-copy A, B, C, and D sequences. Coding sequences of genes are represented as empty boxes, with 5′ and 3′ indicating their orientation. Transposable elements are represented as shaded boxes with pointed ends. The different copies of the known TEs have been numbered sequentially following the order of the copies previously described (Cáceres 2000; Cáceres, Puig, and Ruiz 2001). Some of the TE copies (*BuT5-3*, *BuT5-4*, *Galileo-11*, and one end of *Kepler-5*) are very small (see table 3) and are not drawn to scale. Target site duplications flanking several of the TEs are shown in boxes above them. Thick vertical arrows limit the insertions found at the A–C and B–D junctures. The total size of each insertion is given below. Horizontal arrows represent primers used for PCR amplification. Lines under the sequences indicate probes used for Southern hybridizations. Restriction sites: A: *Xmn* I; B: *Bam* HI; C: *Cla* I; D: *Dra* I; E: *Eco* RI; H: *Hind* III; S: *Sal* I; X: *Xba* I.

hallmarks of what may be considered a new transposon and has been designated *BuT6*, following Cáceres, Puig, and Ruiz (2001). This element is flanked by 8-bp target site duplications and ends with short inverted terminal repeats (ITRs) of 13 bp, similar to those of other Class II elements of the *hAT* superfamily (Calvi et al. 1991). The TE content of the remaining breakpoint insertions is summarized in table 3 and figure 3. Briefly, the 1.8-kb insertion in the A-C junction comprises a truncated copy of the transposon *BuT5* and a *Galileo* element. The 2.4-kb insertion in the B-D junction is made up of three partial copies and one complete copy of *BuT5*, one copy of *Kepler*, and two small sequences corresponding to *Galileo* ends. Finally, the 3-kb D insertion contains one long *Galileo* copy inserted within a *BuT3* element.

Table 3
Transposable Elements Found at the Breakpoint Regions of Inversion $2q^7$ in the jq^7-4 Line of *D. buzzatii*

Breakpoint Region	Transposable Element	Size (bp)	ITR (bp)	Target Site (bp)
A	*BuT6*	387	13	8
A-C	*BuT5-2*	669	ND	ND
A-C	*Galileo-10*	1,139	336/331	7
B-D	*BuT5-3*	8	ND	ND
B-D	*BuT5-4*	33	ND	ND
B-D	*Galileo-11*	20	8	ND
B-D	*BuT5-5*	390	ND	ND
B-D	*Kepler-5*	940	222	ND
B-D	*BuT5-6*	1,041	3	9
D	*BuT3-6*	688	22	8
D	*Galileo-12*	2,304	959/1,115	ND

NOTE.—When different, the sizes of the left and right inverted terminal repeats (ITRs) are indicated. ND, not determined.

Structural Variation of the Inversion $2q^7$ Breakpoint Regions

In addition to the sequencing of the inversion breakpoints in j-19 and jq^7-4, the genomic structure of the breakpoint regions was investigated in 20 other lines without the $2q^7$ inversion (eight *2st* lines, nine *2j* lines, and three $2jz^3$ lines) and in five other lines with the $2q^7$ inversion. The techniques used include Southern blotting, PCR amplification, restriction mapping, and sequencing of PCR products. In the lines without the inversion, two PCR reactions were carried out with primer pairs A1-B1 and C1-D1 to amplify the distal and proximal breakpoint regions, respectively (see fig. 3). In most lines a PCR product of similar size to that generated by the reference line (j-19) was obtained, but st-8, st-9, j-9, j-11, j-12, and j-16 in the A1-B1 PCR and st-3 and j-16 in the C1-D1 PCR produced slightly different amplification bands containing

Table 4
PCR Amplification Analysis of the $2q^7$ Breakpoint Regions in Six $2jq^7$ Chromosomal Lines

	Distal Breakpoint Region (AC)				Proximal Breakpoint Region (BD)				
Line	A1-T1	A1-T2	A1-C1	T3-C1	B1-T4	B1-T5	T8-D1[a]	T3-D1[a]	T9-D1
jq^7-1	**584 bp**	0.9 kb	2.3 kb	**332 bp**	**778 bp**	X	X	X	**671 bp**
jq^7-2	**588 bp**	0.9 kb	2.3 kb	**332 bp**	**778 bp**	X	X	X	**671 bp**
jq^7-3	**588 bp**	0.9 kb	2.3 kb	**332 bp**	**778 bp**	X	X	X	**671 bp**
jq^7-4	**584 bp**	0.9 kb	2.3 kb	**332 bp**	**777 bp**	1.9 kb	1.9 kb	0.8 kb	**671 bp**
jq^7-5	**584 bp**	0.9 kb	2.3 kb	**332 bp**	**777 bp**	1.9 kb	1.9 kb	0.8 kb	**671 bp**
jq^7-6	**567 bp**	X	X	**347 bp**	X	**763 bp**	X	X	**671 bp**

NOTE.—PCR products that were sequenced are shown in boldface. X indicates that no PCR product was obtained. See figure 3 for location of primers.
[a] DNA was digested with *DraI* prior to PCR amplification.

small insertions and/or deletions. One line (jz^3-4) failed to yield any A1-B1 product and by hybridization of *Bam* HI-*Hind* III digested DNA with the AB probe it was shown that it contains a 1.6 kb insertion (probably corresponding to an element of the *Foldback* family, as suggested by the failure of the PCR reaction). The same Southern hybridization also showed that none of the lines without the inversion examined (st-1, st-8, j-1, j-9, j-19, jz^3-1) had the *BuT6* insertion that was present in the A region of all $2jq^7$ lines (see below).

In the lines with the inversion, we performed Southern analysis with AB and CD probes (fig. 3) and PCR amplification of the distal (AC) and proximal (BD) breakpoint regions using different primer pairs (table 1 and fig. 3). In all the amplifications, at least one of the primers in each pair was anchored in single-copy DNA to avoid unspecific amplification. Results of informative PCR reactions and Southern analysis are shown in tables 4 and 5, respectively. In the distal breakpoint region (AC), the *BuT6* insertion was found in all the $2jq^7$ lines and the same 1.8-kb insertion was present at exactly the same position in all $2jq^7$ lines, except in jq^7-6. This line possess a 170-bp deletion in A, lacks two 19-bp and 66-bp *BuT5-2* deletions present in the other $2jq^7$ lines, has an additional copy of the 13-bp right-end sequence of *Galileo-10*, and the AC insertion is ~3 kb larger (figs. 4 and 5). Further structural variability between the $2jq^7$ lines was detected in the proximal breakpoint (BD) region, where four out of five lines showed major differences with jq^7-4. These differences, summarized in figures 4 and 5, basically are these: (1) the substitution of part of the left end of the BD insertion by a different *BuT5* fragment (*BuT5-7*) and the lack of the *BuT5-6* insertion in jq^7-6, and (2) the absence of the *Galileo-12* element and the presence of additional sequences in the central portion of the BD insertion in jq^7-1, jq^7-2, jq^7-3, and jq^7-6.

Nucleotide Variation at the $2q^7$ Breakpoints and Dating of the Inversion

To estimate the nucleotide variation at the breakpoint regions of the $2q^7$ inversion, we sequenced the PCR products obtained with primer pairs A1-B1 and C1-D1 in nine lines without the $2q^7$ inversion and those obtained with primer pairs A1-T1, T3-C1, B1-T4 (B1-T5 in jq^7-6), and T9-D1 in all six $2jq^7$ lines (fig. 5). In addition, the A, B, C, and D regions were also sequenced in *D. koepferae*, a close relative of *D. buzzatii*. All the sequences of A, B, C, and D regions are located in non-coding regions, except for 37 nucleotides of A corresponding to the *snRNA:U1* gene and 35 nucleotides of C corresponding to the *CG1172* gene.

Overall, 86 and 21 segregating sites were found in single-copy DNA regions (ABCD) and the transposable elements sequences, respectively (table 6). In addition, excluding the large TE insertions, there were 11 small insertions (ranging from 1 to 32 nucleotides) and 22 deletions (ranging from 1 to 170 nucleotides) in the A, B, C, and D sequences, and five insertions (ranging from 1 to 66 nucleotides) in the transposable element sequences (fig. 5). Nucleotide diversity (π; Nei 1987) values in the different regions are given in table 6. First, there is a sharp contrast in the nucleotide diversity of the single-copy DNA regions between the non-inverted chromosomes

Table 5
Southern Hybridization Analysis of the $2q^7$ Breakpoint Regions in Six $2jq^7$ Chromosomal Lines

	AB Probe										CD Probe									
	ClaI		DraI		EcoRI		BamHI +HindIII		XmnI		ClaI		DraI		EcoRI		HindIII		XmnI	
Line	AC	BD	AC	BD	AC	BD	AC	BD	AC	BD	AC	BD	AC	BD	AC	BD	AC	BD	AC	BD
jq^7-1	3.5	—	1.3	1.1	5.5	1.3	2	5	6.5	12	3.5	0.6	1.6	1.8	4.2	4.3	2.1	6	6.5	12
jq^7-2	3.5	—	1.3	1.1	5.5	2.3	2	7.1	6.5	13	3.5	0.6	1.6	1.8	4.2	3	2.1	6	6.5	13
jq^7-3	3.5	—	1.3	1.1	5.5	2.3	2	7.1	6.5	13	3.5	0.6	1.6	1.8	4.2	3	2.1	6	6.5	13
jq^7-4	3.5	—	1.3	0.9	5.5	1.5	2	6.1	6.5	4.8	3.5	0.6	1.6	2.5	4.2	1.5	2.1	6	6.5	6.5
jq^7-5	3.5	—	1.3	0.9	5.5	1.5	2	6.1	6.5	4.8	3.5	0.6	1.6	2.5	4.2	1.5	2.1	6	6.5	6.5
jq^7-6	6.5	—	1.1	6	5.5	0.4	2.8	6.5	9.5	3.8	6.5	0.6	1.9	1.8	4.2	3	4.4	6	9.5	8

NOTE.—The sizes of the hybridization bands detected in the distal (AC) and proximal (BD) breakpoint regions for each of the probes and restriction enzymes assayed are given in kb.

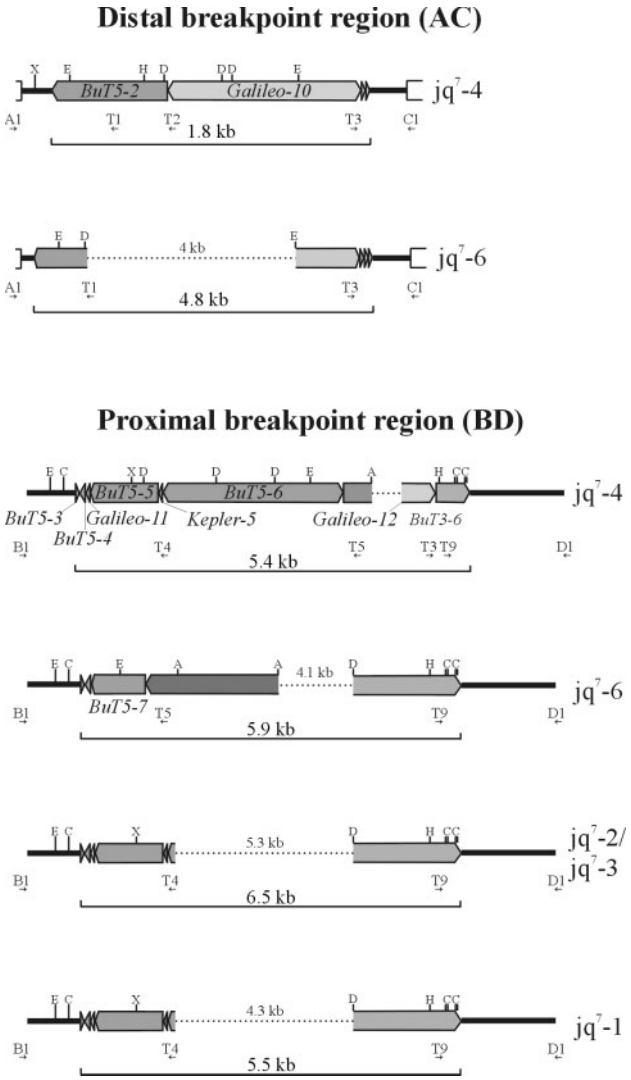

FIG. 4.—Structural variation at the $2q^7$ inversion breakpoint regions in six different $2jq^7$ lines. Partial structures inferred from Southern analysis, PCR amplification, and sequencing are shown only for those lines with differences when compared to line jq^7-4. Dotted lines indicate segments where the exact structure is not known, and the total size of the insertions is given below. Structure in line jq^7-4 is shown as reference. Symbols are as in figure 3.

($\pi = 0.0178$) and those with the $2q^7$ inversion ($\pi = 0$). Based on the heterogeneity test of Kreitman and Hudson (1991), this difference is statistically significant ($\chi^2_L = 29$, df = 1, $P < 0.001$). Second, the level of polymorphism varies between the four single-copy DNA regions (ABCD) of non-inverted chromosomes, with region A exhibiting around four times more nucleotide variation than regions B, C, and D ($\chi^2_L = 24.78$, df = 3, $P < 0.001$). Finally, the distal and proximal breakpoint insertions of inverted chromosomes show much higher nucleotide diversity ($\pi = 0.0125$) than the adjacent single-copy sequences, and this value is more than four times higher in the distal breakpoint insertion than in the proximal breakpoint insertion ($\chi^2_L = 10.45$, df = 2, $P < 0.01$).

No significant departures from the neutral model in the four single-copy regions were found with the Tajima (1989) and Fu and Li (1993) tests. Thus, we used the divergence in these regions between inverted and non-inverted chromosomes to date the origin of the $2q^7$ inversion (Hasson and Eanes 1996; Cáceres, Puig, and Ruiz 2001). The average numbers of nucleotide substitutions per site, d_{xy}, and the net number of nucleotide substitutions per site, d_a, between inverted ($2jq^7$) and non-inverted ($2st$, $2j$, and $2jz^3$) chromosomes are 0.0155 and 0.0066, respectively (Nei 1987). The corresponding values for the comparison between *D. buzzatii* and *D. koepferae*, two species that diverged 4.2 MYA (Russo, Takezaki, and Nei 1995; Rodríguez-Trelles, Alarcón, and Fontdevila 2000), are 0.0748 and 0.0571. We have used as an estimate of the intraspecific nucleotide diversity the π value for non-inverted chromosomes (table 6), because the low frequency of the $2q^7$ inversion and its endemic distribution make its overall contribution to the species diversity negligible. The same value was taken as an estimate for *D. koepferae* intraspecific diversity. A rate of 6.8×10^{-9} nucleotide substitutions per site and per year results, which indicates that the $2q^7$ inversion is 0.49 Myr old. If the A region, which displays a higher polymorphism level, is excluded from the calculations, a rate of 6.25×10^{-9} nucleotide substitutions per site and per year, and an age of 0.67 Myr for inversion $2q^7$ are obtained. Finally, we have used the amount of nucleotide diversity to estimate the age of the sampled $2jq^7$ alleles (Rozas et al. 1999; Cáceres, Puig, and Ruiz 2001). Given that no nucleotide polymorphism has been found in the single-copy DNA regions between the different $2jq^7$ chromosomes, an upper bound for the coalescence time of the $2jq^7$ alleles has been estimated assuming a single nucleotide change in one sequence ($\pi = 0.0003$). Using the two previous rates of nucleotide substitution, this results in a maximum age for the sampled $2jq^7$ alleles between 20,000 years (including the A region) and 25,000 years (excluding the A region).

Discussion

Two different models have been proposed to explain the induction of chromosomal inversions by TEs: the ectopic recombination model (Petes and Hill 1988; Lim and Simmons 1994) and the hybrid element insertion model (Gray 2000). Under the ectopic recombination model, inversions arise by homologous recombination between two copies of the same TE inserted in opposite orientation at different sites of the same chromosome. Thus, the TEs precede the generation of the inversion and serve as (perhaps passive) substrates for the recombination event. Both Class I and Class II elements may participate in ectopic recombination and the cellular machinery involved may be the same operative in regular meiotic recombination (Virgin and Bailey 1998). The outcome is an inversion flanked by a pair of TE copies that have their original target site duplications, aa and bb, exchanged to give the arrangement ab′ and a′b (where a′ and b′ designate the inverted and complementary versions of sequences a and b, respectively). Transposable elements may also induce inversions by a different mechanism, called the hybrid element insertion model (Gray 2000). Under this model, a single TE insertion results, after DNA

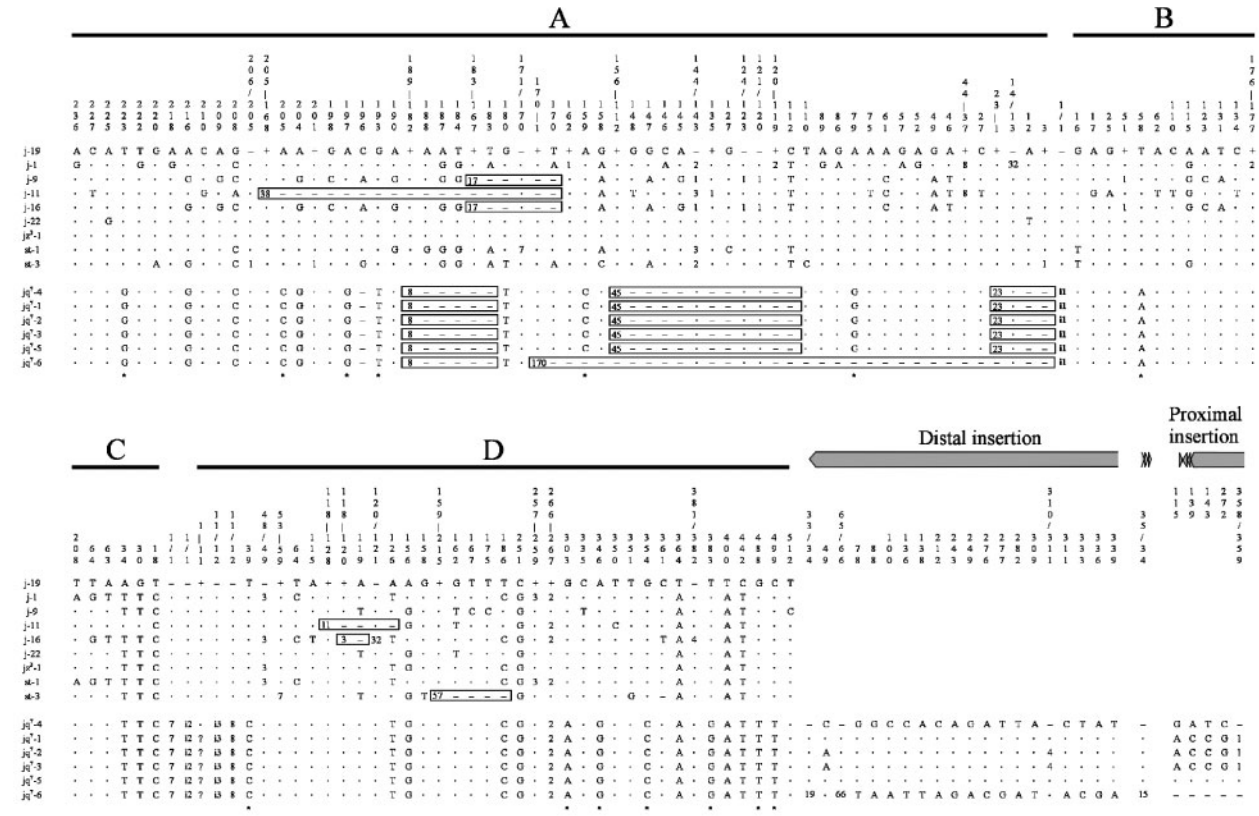

FIG. 5.—Nucleotide polymorphism at the breakpoint regions of the inversion $2q^7$. For each region, nucleotide positions are numbered taking the breakpoints as start points. For convenience, the 23 nucleotides located between A and B regions in non-inverted chromosomes that have not been found in inverted chromosomes, are included in the A sequence. j-19 sequence is taken as reference for the A, B, C, and D regions, and jq^7-4 is taken as reference for the breakpoint insertions. Positions with nucleotides identical to the reference sequence are indicated by a dot. Insertions and deletions are represented by minus and plus signs in the reference sequence, respectively, and a number in the line with the insertion or deletion indicating its size in nucleotides. Deletions including more than one position of the reference line are included in rectangles. Question marks indicate missing data. TE insertions found at the proximal and distal breakpoints in inverted chromosomes are indicated as i1 and i2, and the insertion found in region D as i3. Asterisks indicate positions with fixed nucleotide differences between inverted and non-inverted chromosomes.

replication, in two TE copies inserted at the same site in sister chromatids. These two copies may participate in an aberrant transposition event, by which a hybrid element formed by one end of the first copy and the opposite end of the second copy transposes to a new chromosomal site. The outcome is an inversion of the segment between the two chromosomal sites flanked by two TE copies, which originated by DNA replication and are initially identical. The arrangement of the target site duplications flanking the TE copies will be the same as in the ectopic recombination model (see above). Thus, the outcomes of the two models are strikingly similar, except perhaps for the fact that the two TE copies involved in recombination may differ, yielding chimerical elements, whereas those resulting from the aberrant transposition of a hybrid element must be identical, at least shortly after the origin of the inversion.

The location of the insertions of 1.8 kb and 2.4 kb directly into the A-C and B-D junctures, respectively, points to their involvement in the origin of the inversion (see below). The other two insertions at the breakpoint regions are not directly involved in the generation of the $2q^7$ inversion and were seemingly caused by secondary TE invaders, as shown by the direct target site duplications flanking *BuT6* in region A and *BuT3-6* in region D. Among the inserted TEs, the *Foldback*-like transposon *Galileo* is the most likely inducer of the $2q^7$ inversion. One long copy of *Galileo* is found at the A-C junction (*Galileo-10*) and two small *Galileo* end fragments are found at the B-D junction (*Galileo-11*) (fig. 3). *Galileo* duplicates 7 nucleotides of the target site upon insertion (Cáceres, Puig, and Ruiz 2001), and as expected if *Galileo* originated the $2q^7$ inversion, the 7-bp sequence flanking *Galileo-10* in region C (GAACAAG) is the inverted and complementary version of the 7-bp sequence flanking *Galileo-11* in region D. The 7-bp sequence at the other end of *Galileo-10* (GTTATAC) fits well with the consensus target sequence ($G_{10}T_{11}a_8g_7T_{11}A_{13}c_6$) proposed for *Galileo* and two other *D. buzzatii Foldback*-like elements, *Kepler* and *Newton* (Cáceres 2000). This 7-bp sequence pertains to *BuT5-2*, which suggests that *Galileo-10* inserted originally within a pre-existing *BuT5* element. Neither the complementary 7-bp sequence nor the remaining fragment of *BuT5-2* were found at the other end of *Galileo-11* in region B, as would be expected for the ectopic recombination and hybrid element insertion models. However, because the BD region bears the largest number of insertions and structural changes, the most likely explanation is that a deletion removed the 7-bp duplication along with the *BuT5-2*

Table 6
Nucleotide Variation at the Breakpoints Regions of the $2q^7$ Inversion

		Non-inverted Chromosomes (n = 9)		Inverted Chromosomes (n = 6)	
Region	m	S	π	S	π
ABCD	1420	86	0.0178	0	0
A	326	44	0.0472	0	0
B	285	10	0.0100	0	0
C	250	6	0.0096	0	0
D	559	26	0.0110	0	0
Insertions	1040	—	—	21	0.0125
Distal	483	—	—	17	0.0155
Proximal	450	—	—	4	0.0036
D	107	—	—	0	0

NOTE.—n: number of sequences; m: number of nucleotides; S: number of segregating sites; π: nucleotide diversity.

Table 7
Divergence Between the Last 336 Nucleotides of the ITRs of Four *Galileo* Elements

	3a	3b	4a	4b	10a	10b	12a	12b
3a	0	**0**	0.0298	0.0298	0.0387	0.0273	0.0208	0.0149
3b		0	0.0298	0.0298	0.0387	0.0273	0.0208	0.0149
4a			0	**0**	0.0506	0.0303	0.0089	0.0149
4b				0	0.0506	0.0303	0.0089	0.0149
10a					0	**0.0364**	0.0417	0.0357
10b						0	0.0212	0.0212
12a							0	**0.0060**
12b								0

NOTE.—The number indicates the *Galileo* copy, and a and b correspond to the two ITRs of the same element; values in boldface correspond to the comparisons between ITRs of the same element.

sequences. This deletion could also have removed the 23 nucleotides of the AB sequence that are not present in the chromosomes with the inversion.

Additional evidence supports the role of *Galileo* in the origin of the $2q^7$ inversion and suggests that ectopic recombination may be the actual mechanism involved: *Galileo-10* seems to be a chimerical element that was probably generated by recombination between two slightly different *Galileo* copies. We have compared the sequence of the inverted terminal repeats (ITRs) at both ends of *Galileo-10* with the corresponding sequences of *Galileo-12* and two other *Galileo* copies described previously, *Galileo-3* and *Galileo-4* (Cáceres, Puig, and Ruiz 2001). The ITRs from the same element always exhibit much less sequence divergence than those of different elements (table 7). The exception is *Galileo-10,* whose ITRs show a degree of divergence similar to that observed between ITRs from different elements and six times higher than between ITRs belonging to the same element. Although the differences between the two ITRs of *Galileo-10* may also have arisen by mutation, the mutation rate should be exceedingly high to account for such level of divergence. Thus the likely chimerical nature of *Galileo-10* provides support for the ectopic recombination model. Similarly, the comparison between the long terminal repeats (LTR) of endogenous retroviruses (HERVs) and the target site duplications flanking them has been employed as an indicator of genomic rearrangements occurring through ectopic recombination in humans (Hughes and Coffin 2001).

A high frequency of TE insertions and other structural changes has been detected at the $2q^7$ inversion breakpoints. This amount of structural variability is surprising if we consider that we have not found any nucleotide polymorphism in the $2jq^7$ chromosomes. The structural differences between the six studied lines should have arisen in a very short period of time, because the age of the alleles has been estimated to be less than 25,000 years. Both estimates of the age of the $2q^7$ inversion (0.49–0.67 Myr) and of the sampled alleles (20,000–25,000 years) are consistent with those calculated for the *2j* inversion, ~1 Myr and 83,000 years, respectively (Cáceres, Puig, and Ruiz 2001), from which the $2q^7$ inversion arose. In addition, the lack of nucleotide polymorphism and the young age for the alleles are features consistent with the low frequencies of the inversion in the natural populations of *D. buzzatii* (Hasson et al. 1995). It is noteworthy that a similar degree of structural variability was found at the *2j* inversion breakpoints (Cáceres, Puig, and Ruiz 2001), and thus the four inversion breakpoints sequenced in *D. buzzatii* have in common the presence of *Galileo* elements and the fact that they seem to be hotspots for TE insertions and other structural changes. It has been proposed that TEs should accumulate in low-recombination regions owing to a low rate of elimination by ectopic recombination (Charlesworth, Sniegowski, and Stephan 1994; Sniegowski and Charlesworth 1994), and the distribution of TEs in the recently sequenced genome of *D. melanogaster* (Adams et al. 2000) provides support for this hypothesis (Rizzon et al. 2002; Bartolomé, Maside, and Charlesworth 2002). Thus an accumulation of TEs is expected near the inversion breakpoints because of the reduction of recombination in these regions in inversion heterokaryotypes (Eanes, Wesley, and Charlesworth 1992; Sniegowski and Charlesworth 1994). This effect can certainly account in part for the TE clusters found at *D. buzzatii* inversion breakpoints (Cáceres, Puig, and Ruiz 2001, this work). However, we think that the particular properties of the *Foldback*-like *Galileo* elements may also be involved in the observed structural instability.

In *D. melanogaster Foldback* elements are known to give rise to genetic instability and promote different types of recombination processes (Levis, Collins, and Rubin 1982; Bingham and Zachar 1989; Smith and Corces 1991). These elements generate deletions, inversions, and reciprocal translocations at high frequencies, apparently through ectopic recombination (Collins and Rubin 1984); they show a high frequency of excision (Collins and Rubin 1983); and they usually harbor other TE insertions (Brierley and Potter 1985; Harden and Ashburner 1990). The capacity for generating rearrangements of these elements through recombination processes is probably increased by the presence of very long ITRs. Palindromic sequences, such as ITRs, have been demonstrated to be a source of genomic instability, causing different types of chromosomal rearrangements in a wide variety of organisms (Zhou, Akgün, and Jasin 2001). The number of rearrangements increases with the length of the ITRs and decreases with the size of the internal sequence, and it

is probably related to its ability to form secondary structures and give rise to double-strand breaks (Lobachev et al. 1998). The size of the ITRs of the most complete described copies of *Galileo* varies between 683 bp (*Galileo-3*) and 1115 bp (*Galileo-12*) (Cáceres, Puig, and Ruiz 2001; this work) and, together with the length of the spacer DNA between them, are among those expected to produce the larger increases in the number of rearrangements. The capacity of *D. melanogaster Foldback* elements to form secondary structures when denatured was early demonstrated (Truett, Jones, and Potter 1981), and in the case of *Galileo* and related elements this ability is exemplified by the difficulties encountered during their amplification by PCR (Cáceres, Puig, and Ruiz 2001; this work).

The *Galileo* element of *D. buzzatii* has seemingly originated the two polymorphic inversions *2j* and $2q^7$ of this species studied to date. Moreover, the four inversion breakpoints appear to have become genetically unstable regions and hotspots for the accumulation of TE insertions and other structural changes. These observations suggest that *Galileo* is an active element that may play an important role in the genome evolution of *D. buzzatii* and related species. Future studies of the chromosomal distribution of the TEs found at the inversion breakpoints will help to answer some questions regarding the copy number and distribution of these elements in the *D. buzzatii* genome, their association to other low recombination regions apart from inversion breakpoints, and the existence or not of similar hotspots in other chromosomal regions.

Acknowledgments

We thank E. Hasson and J. S. F. Barker for supplying *D. buzzatii* lines, and J. González and J. M. Ranz for advice and technical support. This work was supported by grant PB98-0900-C02-01 from the Dirección General de Enseñanza Superior e Investigación Científica (Ministerio de Educación y Cultura, Spain) awarded to A.R., and by a doctoral FI fellowship from the Universitat Autònoma de Barcelona awarded to F.C.

Literature Cited

Adams, M. D., S. E. Celniker, and R. A. Holt et al. (192 co-authors). 2000. The genome sequence of *Drosophila melanogaster*. Science **287**:2185–2195.

Andolfatto, P., J. D. Wall, and M. Kreitman. 1999. Unusual haplotype structure at the proximal breakpoint of *In(2L)t* in a natural population of *Drosophila melanogaster*. Genetics **153**:1297–1311.

Bartolomé, C., X. Maside, and B. Charlesworth. 2002. On the abundance and distribution of transposable elements in the genome of *Drosophila melanogaster*. Mol. Biol. Evol. **19**: 926–937.

Berg, D. E., and M. M. Howe. 1989. Mobile DNA. American Society for Microbiology, Washington, D.C.

Bingham, P. M., and Z. Zachar. 1989. Retrotransposons and the *FB* transposon from *Drosophila melanogaster*. Pp. 485–502 *in* D. E. Berg and M. M. Howe, eds. Mobile DNA. American Society for Microbiology, Washington, D.C.

Brierley, H. L., and S. S. Potter. 1985. Distinct characteristics of loop sequences of two Drosophila foldback transposable elements. Nucleic Acids Res. **13**:485–500.

Cáceres, M. 2000. Inversiones cromosómicas en Drosophila: origen molecular y significado evolutivo de su tamaño. Ph.D. thesis, Universitat Autònoma de Barcelona, Bellaterra (Barcelona), Spain.

Cáceres, M., M. Puig, and A. Ruiz. 2001. Molecular characterization of two natural hotspots in the Drosophila genome induced by transposon insertions. Genome Res. **11**:1353–1364.

Cáceres, M., J. M. Ranz, A. Barbadilla, M. Long, and A. Ruiz. 1999. Generation of a widespread Drosophila inversion by a transposable element. Science **285**:415–418.

Calvi, B. R., T. J. Hong, S. D. Findley, and W. M. Gelbart. 1991. Evidence for a common evolutionary origin of inverted repeat transposons in Drosophila and plants: *hobo*, *Activator*, and *Tam3*. Cell **66**:465–471.

Charlesworth, B., P. Sniegowski, and W. Stephan. 1994. The evolutionary dynamics of repetitive DNA in eukaryotes. Nature **371**:215–220.

Cirera, S., J. M. Martín-Campos, C. Segarra, and M. Aguadé. 1995. Molecular characterization of the breakpoints of an inversion fixed between *Drosophila melanogaster* and *D. subobscura*. Genetics **139**:321–326.

Collins, M., and G. M. Rubin. 1983. High-frequency precise excision of the Drosophila *foldback* transposable element. Nature **303**:259–260.

———. 1984. Structure of chromosomal rearrangements induced by the *FB* transposable element in Drosophila. Nature **308**: 323–327.

Daveran-Mingot, M.-L., N. Campo, P. Ritzenthaler, and P. le Bourgeois. 1998. A natural large chromosomal inversion in *Lactococcus lactis* is mediated by homologous recombination between two insertion sequences. J. Bacteriol. **180**:4834–4842.

Eanes, W. F., C. Wesley, and B. Charlesworth. 1992. Accumulation of P elements in minority inversions in natural populations of *Drosophila melanogaster*. Genet. Res. **59**:1–9.

Evgen'ev, M. B., H. Zelentsova, H. Poluectova, G. T. Lyozin, V. Veleikodvorskaja, K. I. Pyatkov, L. A. Zhivotovsky, and M. G. Kidwell. 2000. Mobile elements and chromosomal evolution in the virilis group of Drosophila. Proc. Natl. Acad. Sci. USA **97**:11337–11342.

Finnegan, D. J. 1989. Eukaryotic transposable elements and genome evolution. Trends Genet. **5**:103–107.

Fu, Y.-X., and W.-H. Li. 1993. Statistical tests of neutrality of mutations. Genetics **133**:693–709.

González, J., J. M. Ranz, and A. Ruiz. 2002. Chromosomal elements evolve at different rates in the Drosophila genome. Genetics **161**:1137–1154.

Gray, Y. H. M. 2000. It takes two transposons to tango. Transposable-element mediated chromosomal rearrangements. Trends Genet. **16**:461–468.

Grosshans, J., F. Schnorrer, and C. Nusslein-Volhard. 1999. Oligomerisation of tube and pelle leads to nuclear localisation of dorsal. Mech. Dev. **81**:127–138.

Harden, N., and M. Ashburner. 1990. Characterization of the *FOB-NOF* transposable element of *Drosophila melanogaster*. Genetics **126**:387–400.

Hasson, E., and W. F. Eanes. 1996. Contrasting histories of three gene regions associated with *In(3L)Payne* of *Drosophila melanogaster*. Genetics **144**:1565–1575.

Hasson, E., C. Rodríguez, J. J. Fanara, H. Naveira, O. A. Reig, and A. Fontdevila. 1995. The evolutionary history of *Drosophila buzzatii*. XXVI. Macrogeographic patterns of inversion polymorphism in New World populations. J. Evol. Biol. **8**:369–384.

Heino, T. I., A. O. Saura, and V. Sorsa. 1994. Maps of the salivary gland chromosomes of *Drosophila melanogaster*. Dros. Inform. Serv. **73**:621–738.

Hughes, J. F., and J. M. Coffin. 2001. Evidence for genomic rearrangements mediated by human endogenous retroviruses during primate evolution. Nat. Genet. **29**:487–489.

Kim, J. M., S. Vanguri, J. D. Boeke, A. Gabriel, and D. F. Voytas. 1998. Transposable elements and genome organization: a comprehensive survey of retrotransposons revealed by the complete *Saccharomyces cerevisiae* genome sequence. Genome Res. **8**:464–478.

Kreitman, M., and R. R. Hudson. 1991. Inferring the evolutionary histories of the *Adh* and *Adh-dup* loci in *Drosophila melanogaster* from patterns of polymorphism and divergence. Genetics **127**:565–582.

Krimbas, C. B., and J. R. Powell. 1992. Drosophila inversion polymorphism. CRC Press, Boca Raton, Fla.

Lefevre, G. Jr. 1976. A photoghraphyc representation and interpretation of the polytene chromosomes of *Drosophila melanogaster* salivary glands. Pp. 31–36 *in* M. Ashburner, H. L. Carson, and J. N. Thompson, eds. The genetics and biology of Drosophila. Academic Press, London.

Levis, R., M. Collins, and G. M. Rubin. 1982. FB elements are the common basis for the instability of the w^{DZL} and w^{c} Drosophila mutations. Cell **30**:551–565.

Lim, J. K., and M. J. Simmons. 1994. Gross chromosome rearrangements mediated by transposable elements in *Drosophila melanogaster*. Bioessays **16**:269–275.

Lobachev, K. S., B. M. Shor, H. T. Tran, W. Taylor, J. D. Keen, M. A. Resnick, and D. A. Gordenin. 1998. Factors affecting inverted repeat stimulation of recombination and deletion in *Saccharomyces cerevisiae*. 1998. Genetics **148**:1507–1524.

Lyttle, T. W., and D. S. Haymer. 1992. The role of the transposable element *hobo* in the origin of endemic inversions in wild populations of *Drosophila melanogaster*. Genetica **86**:113–126.

Mathiopoulos, K. D., A. della Torre, V. Predazzi, V. Petrarca, and M. Coluzzi. 1998. Cloning of inversion breakpoints in the *Anopheles gambiae* complex traces a transposable element at the inversion junction. Proc. Natl. Acad. Sci. USA **95**:12444–12449.

McDonald, J. F. 1993. Evolution and consequences of transposable elements. Curr. Opin. Genet. Dev. **3**:855–864.

Montgomery, E., B. Charlesworth, and C. H. Langley. 1987. A test for role of natural selection in the stabilization of transposable element copy number in a population of *Drosophila melanogaster*. Genet. Res. **49**:31–41.

Nei, M. 1987. Molecular evolutionary genetics. Columbia University Press, New York.

Petes, T. D., and C. W. Hill. 1988. Recombination between repeated genes in microorganisms. Annu. Rev. Genet. **22**:147–168.

Powell, J. R. 1997. Progress and prospects in evolutionary biology: the Drosophila model. Oxford University Press, New York.

Ranz, J. M., F. Casals, and A. Ruiz. 2001. How malleable is the eukaryotic genome? Extreme rate of chromosomal rearrangement in the genus Drosophila. Genome Res. **11**: 230–239.

Regner, L. P., M. S. O. Pereira, C. E. V. Alonso, E. Abdelhay, and V. L. S. Valente. 1996. Genomic distribution of *P* elements in *Drosophila willistoni* and a search for their relationship with chromosomal inversions. J. Hered. **87**:191–198.

Rizzon, C., G. Marais, M. Gouy, and C. Biemont. 2002. Recombination rate and the distribution of transposable elements in the *Drosophila melanogaster* genome. Genome Res. **12**:400–407.

Rodríguez-Trelles, F., L. Alarcón, and A. Fontdevila. 2000. Molecular evolution of the *buzzatii* complex (*Drosophila repleta* group): a maximum-likelihood approach. Mol. Biol. Evol. **17**:1112–1122.

Rozas, J., and R. Rozas. 1999. DnaSP version 3: an integrated program for molecular population genetics and molecular evolution analysis. Bioinformatics **15**:174–175.

Rozas, J., C. Segarra, G. Ribó, and M. Aguadé. 1999. Molecular population genetics of the *rp49* gene region in different chromosomal inversions of *Drosophila subobscura*. Genetics **151**:189–202.

Ruiz, A., and M. Wasserman. 1993. Evolutionary cytogenetics of the *Drosophila buzzatii* species complex. Heredity **70**:582–596.

Russo, C.A.M., N. Takezaki, and M. Nei. 1995. Molecular phylogeny and divergence times of drosophilid species. Mol. Biol. Evol. **4**:406–425.

Sambrook, J., E. F. Fritsch, and T. Maniatis. 1989. Molecular cloning, a laboratory manual. Cold Spring Harbor Laboratory Press, Cold Spring Harbor, N.Y.

Schwartz, A., D. C. Chan, L. G. Brown, R. Alagappan, D. Pettay, C. Disteche, B. McGillivray, A. de la Chapelle, and D. C. Page. 1998. Reconstructing hominid Y evolution: X-homologous block, created by X-Y transposition, was disrupted by Yp inversion through LINE-LINE recombination. Hum. Mol. Genet. **7**:1–11.

Segarra, C., E. R. Lozovskaya, G. Ribó, M. Agaudé, and D. L. Hartl. 1995. P1 clones from *Drosophila melanogaster* as markers to study the chromosomal evolution of Muller's A element in two species of the obscura group of Drosophila. Chromosoma **104**:129–136.

Smith, P. A., and V. G. Corces. 1991. Drosophila transposable elements: mechanisms of mutagenesis and interactions with the host genome. Adv. Genet. **29**:229–300.

Sniegowski, P. D., and B. Charlesworth. 1994. Transposable element numbers in cosmopolitan inversions from a natural population of *Drosophila melanogaster*. Genetics **137**:815–827.

Sperlich, D., and P. Pfriem. 1986. Chromosomal polymorphism in natural and experimental populations. Pp. 257–309 *in* M. Ashburner, H. L. Carson, and J. N. Thompson, eds. The genetics and biology of Drosophila. Vol. 3. Academic Press, London.

Tajima, F. 1989. Statistical method for testing the neutral mutation hypothesis by DNA polymorphism. Genetics **123**: 585–595.

Thompson, J. D., D. G. Higgins, and T. J. Gibson. 1994. Clustal W: improving the sensitivity of progressive multiple sequence alignment through sequence weighting, position-specific gap penalties and weight matrix choice. Nucleic Acids Res. **22**:4673–4680.

Truett, M. A., R. S. Jones, and S. S. Potter. 1981. Unusual structure of the *FB* family of transposable elements in Drosophila. Cell **24**:753–763.

Virgin, J. B., and J. P. Bailey. 1998. The *M26* hotspot of *Schizosaccharomyces pombe* stimulates meiotic ectopic recombination and chromosomal rearrangements. Genetics **149**:1191–1204.

Wesley, C. S., and W. F. Eanes. 1994. Isolation and analysis of the breakpoint sequences of chromosome inversion *In(3L) Payne* in *Drosophila melanogaster*. Evolution **91**:3132–3136.

Zelentsova, H., H. Poluectova, L. Mnjoian, G. Lyozin, V. Veleikodvorskaja, L. Zhivotovsky, M. G. Kidwell, and M. B. Evgen'ev. 1999. Distribution and evolution of mobile elements in the *virilis* species group of Drosophila. Chromosoma **108**:443–56.

Zhou, Z-H., E. Akgün, and M. Jasin. 2001. Repeat expansion by homologous recombination in the mouse germ line at palindromic sequences. Proc. Natl. Acad. Sci USA **98**:8326–8333.

Peer Bork, Associate Editor

Accepted December 10, 2002

3.3 Abundància i distribució cromosòmica dels elements transposables a *D. buzzatii*

Les regions dels punts de trencament de les inversions *2j* i *2q*[7] de *D. buzzatii* contenen vàries insercions d'elements transposables (Cáceres *et al*. 1999b; Cáceres *et al*. 2001; aquest treball). Posteriorment també s'han trobat còpies d'alguns d'aquests elements (*Galileo*, *Kepler*, *BuT4* i *ISBu2*) fora de les regions dels punt de trencament (Cáceres 2000; Negre *et al*. 2003; aquest treball). A la Taula 12 es resumeixen les característiques d'aquests elements.

Taula 12. Resum de les característiques dels elements transposables trobats als punts de trencament de les inversions *2j* i *2jq*[7].

Element	Nº de còpies[a]	Mida mitja (pb)	Còpia més gran (pb)	Referències
		Tipus *Foldback*		
Galileo	12 (6)	1.596	2.304	(1-4)
Kepler	4 (3)	785	940	(2-4)
Newton	2 (2)	1.511	1.512	(3, 4)
		Tipus *hobo*, *Activator*, *Tam 3* (*hAT*)		
BuT1	1 (1)	801	801	(3)
BuT2	1 (1)	2.775	2.775	(3)
BuT3	6 (5)	709	844	(3, 4)
BuT4	2 (2)	721	721	(3, 4)
BuT6	1 (1)	387	387	(4)
		No classificats		
BuT5	6 (2)	1.040	1.041	(3, 4)
ISBu1 [b]	3	1.053	1.467	(3)
ISBu2 [b]	2 (1)	725	725	(3, 5)

[a] Entre parèntesi s'indica el número de còpies utilitzades per calcular la mida mitja (les que inclouen seqüències dels dos ITRs i de la regió interna).
[b] Wilder i Hollocher (2001) han classificat aquests elements dins de la classe I.
(1) Cáceres *et al*. 1999b; (2) Cáceres 2.000; (3) Cáceres *et al*. 2001; (4) Aquest treball; (5) Negre *et al*. 2003.

S'han obtingut sondes de *BuT1*, *BuT2*, *BuT3*, *BuT4*, *BuT5*, *BuT6* i *Galileo*. Amb aquestes sondes s'ha estudiat la distribució d'aquests elements transposables a *D. buzzatii* mitjançant *Southern blotting* i hibridació *in situ*. No s'ha estudiat la distribució dels elements *ISBu-1* i *ISBu-2*, degut a què tenen un nombre mol elevat de còpies i tenyeixen la majoria de les bandes cromosòmiques en les hibridacions *in situ* (Ranz, comunicació personal).

3.3.1 Obtenció de les sondes dels elements transposables

Les sondes s'han obtingut per PCR amb oligonucleòtids localitzats als extrems dels elements (Taula 8 a Material i Mètodes). En el cas dels elements *BuT3* i *BuT4* s'ha utilitzat només un *primer*, ja que les seqüències dels extrems dels elements que cobreixen els oligonucleòtids són molt similars i estan invertides. Les PCRs es van fer sobre DNA de clons de seqüència coneguda, obtinguts durant el procediment de clonació de les insercions trobades als punts de trencament de les inversions *2j* i *2jq*^{7} (Cáceres, comunicació personal; aquest treball), excepte en el cas de *BuT4*. En tots els casos es va obtenir un producte de la mida esperada, i els productes de PCR es van clonar en un vector pGEM-T (Taula 13).

L'element *BuT4* s'ha trobat al punt de trencament distal de la inversió *2j* de tres soques portadores de la inversió (Cáceres *et al*. 2001). A dues d'elles, j-10 i j-19, només hi ha un petit fragment d'un dels extrems de l'element, mentre que a j-9 l'element té els dos extrems però conté una inserció d'un altre element. Per aconseguir una còpia de l'element sense insercions es va fer una PCR sobre DNA genòmic de la soca st-1. Aquesta soca presenta l'ordenació estàndard i no conté cap element trasposable als punts de trencament de les inversions *2j* i *2q*^{7} (Cáceres *et al*. 2001; aquest treball). Es va obtenir un producte amb una mida similar a la de l'element *BuT4-1* sense la inserció (721 pb). Aquest producte es va seqüenciar, confirmant-se que es tracta d'una nova còpia de l'element (*BuT4-2*) de 720 pb.

En el cas de *Galileo* es va digerir el DNA amb l'enzim *DraI* abans de fer la PCR. Les repeticions terminals invertides (ITR) dels element de tipus *Foldback* s'aparellen formant estructures secundàries (Truett *et al*. 1981), que dificulten o impossibiliten l'amplificació per PCR (Cáceres *et al*. 2001; aquest treball). A més, el clon utilitzat (pGPE208), conté pràcticament la totalitat de les dues insercions trobades al punt de trencament proximal de la inversió *2q*^{7}(aquest treball). L'oligonucleòtid E14

està situat just a l'extrem de *Galileo*, i per tant es pot unir als dos extrems de *Galileo-11*, *Galileo-12* i *Kepler-5*, ja que els primers nucleòtids dels seus ITR són idèntics als de *Galileo*. L'oligonucleòtid T8 està situat a la zona intermitja de *Galileo*, que no es troba a *Galileo-11* ni a *Kepler-5* (Figura 3 de l'apartat 3.2, Casals *et al*. 2003). *Galileo-12* conté una diana *DraI* aproximadament a la meitat de l'element, i per tant separa els dos ITR de manera que ja no poden aparellar-se i formar l'estructura secundària. El producte obtingut va ser de la mida esperada i conté la totalitat de l'ITR i part de la regió central de l'element. Els ITR de *Galileo-12* (2.304 pb) tenen 959 i 1.115 pb (aquest treball), i per tant la major part de l'element està continguda en aquesta sonda. L'element *Galileo* té una alta homologia amb dos elements del tipus *Foldback* (*Kepler* i *Newton*) descrits a *D. buzzatii* (Cáceres 2000; Cáceres *et al*. 2001). S'ha comprovat experimentalment que la sonda de *Galileo* utilitzada reconeix aquests dos elements tant en el *Southern* (Manfrin, comunicació personal) com en la hibridació *in situ*. Per tant, les dades sobre la distribució fan referència als tres elements conjuntament.

Taula 13. Característiques de les sondes dels elements transposables.

Element	Mida (pb)	Soca	Punt de trencament	Clon d'origen	Oligonucl. PCR	Clon del producte
BuT1[(1)]	769	j-1	Proximal, inv. *2j*	pGPE109	E1/E2	pGPE220
BuT2[(1)]	2.755	j-8	Proximal, inv. *2j*	pGPE156	E3/E4	pGPE221
BuT3-4[(1)]	795	jq^7-2	Distal, inv. *2j*	pGPE142	E6	pGPE222
BuT4-2[(2)]	720	st-1	-	Genòmic	E8	pGPE224
BuT5-1[(1)]	1.039	jz^3-1	Proximal, inv. *2j*	pGPE129	E9/E10	pGPE225
BuT6[(2)]	387	jq^7-4	Distal, inv. $2jq^7$	pGPE209	E11/E12	pGPE223
Galileo-12[(2)]	1.144	jq^7-4	Proximal inv. $2jq^7$	pGPE208	T8/E14	pGPE226

[(1)] Cáceres *et al*. 2001; [(2)]Aquest treball.

3.3.2 *Southern blotting*

El *Southern blotting* s'ha realitzat sobre DNA genòmic digerit amb dos enzims de restricció de les següents soques: st-1, st-3, st-10, st-11, j-2, j-9, j-19, j-23, j-24, jq^7-1, jq^7-4, jz^3-6, jz^3-7, y^3-1 i s-1. Aquestes soques tenen diferents reordenacions cromosòmiques (Taula 6 a Material i Mètodes). Per cada element transposable s'han utilitzat enzims sense dianes de restricció a cap còpia seqüenciada de l'element. Els enzims són: *EcoRI*/*HindIII* (*BuT1* i *Galileo*), *SalI*/*XbaI* (BuT2), *BamHI*/*EcoRI* (*BuT3* i *BuT4*), *BamHI*/*ClaI* (*BuT5*) i *BamHI*/*HindIII* (*BuT6*). La Figura 10 mostra el resultat de les hibridacions. Les diferències d'intensitat entre les bandes de diferents soques es deuen en alguns casos a diferències en la quantitat de DNA utilitzada. A la Taula 14 es mostra el número de bandes revelades per cada sonda. El número total de bandes de les diferents soques varia entre 89 (y^3-1) i 116 (st-1), però no s'han trobat diferències significatives en el número de còpies totals i de cadascun dels set elements presents a les diferents soques (prova de χ^2). El número mig de bandes per element varia entre 6,93 (*BuT2*) i 26,73 (*Galileo*), i existeixen diferències significatives en l'abundància dels diferents elements ($\chi^2 = 20{,}54$; g. l. = 6; P = 0,002).

3.3.3 Hibridació *in situ*

Les hibridacions *in situ* s'han realitzat sobre cromosomes de les següents soques: st-1, j-2, j-23, j-24, jz^3-6, jz^3-7, jq^7-4, y^3-1, i s-1. A la soca s-1 la inversió *4s* no es troba fixada com s'esperava. Les hibridacions sobre cromosomes d'aquesta soca es van fer sobre heterocariotips. Els número de senyals obtinguts en les hibridacions *in situ* es mostren a la Taula 15. A la Figura 11 i la Taula 16 es mostra la localització dels senyals obtinguts amb cada element a les diferents soques. A la Figura 12 es mostren algunes fotografies de les hibridacions. El nombre de senyals obtinguts a les diferents soques mostra diferències significatives pels elements *BuT1* ($\chi^2 = 22{,}89$; g. l. = 8; P = 0,004), *BuT2* ($\chi^2 = 49{,}1$; g. l. = 8; P < 0,001), *BuT3* ($\chi^2 = 21{,}5$; g. l. = 8; P = 0,006), *BuT5* ($\chi^2 = 54{,}61$; g. l. = 8; P < 0,001), i *BuT6* ($\chi^2 = 21$; g. l. = 8; P = 0,007), així com per al total dels elements ($\chi^2 = 42{,}19$; g. l. = 8; P < 0,001). El número mig de senyals per element varia entre 1,67 (*BuT2*) i 56,11 (*Galileo*), i existeixen diferències significatives en l'abundància dels diferents elements ($\chi^2 = 159{,}09$; g. l. = 6; P < 0,001).

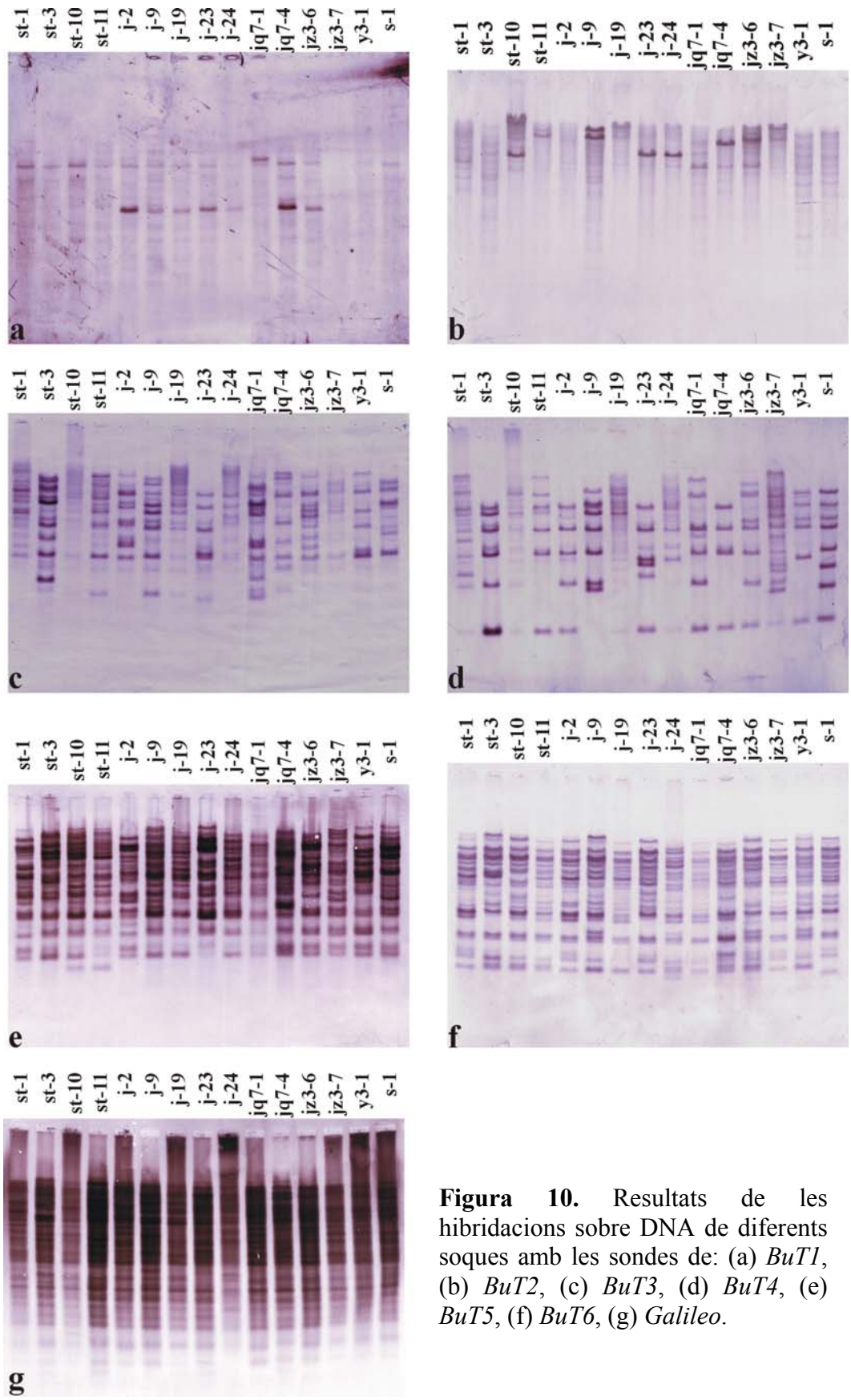

Figura 10. Resultats de les hibridacions sobre DNA de diferents soques amb les sondes de: (a) *BuT1*, (b) *BuT2*, (c) *BuT3*, (d) *BuT4*, (e) *BuT5*, (f) *BuT6*, (g) *Galileo*.

Taula 14. Número de bandes obtingudes en el *Southern blotting* amb les diferents sondes i soques.

Element	st-1	st-3	st-7	st-10	j-2	j-9	j-19	j-23	j-24	jq^7-1	jq^7-4	jz^3-6	jz^3-7	y^3-1	s-1	Mitja
BuT1	11	13	8	15	9	13	11	10	5	10	9	12	5	5	7	9,53
BuT2	7	12	6	6	4	12	7	3	6	7	5	6	5	10	8	6,93
BuT3	15	13	9	15	12	13	13	9	7	14	11	9	6	8	9	10,87
BuT4	15	8	13	10	9	7	13	8	11	8	4	7	16	7	9	9,67
BuT5	19	17	20	21	18	18	17	15	17	17	16	14	19	18	19	17,67
BuT6	20	17	18	18	20	19	18	17	20	15	17	19	18	20	20	18,4
Galileo	29	28	22	27	29	29	29	28	27	28	29	26	25	21	24	26,73
Total	116	108	96	112	101	111	108	90	93	99	91	93	94	89	96	99,8

Taula 15. Número total de senyals d'hibridació produïts per les diferents sondes a cada soca.

Element	st-1	j-2	j-23	j-24	jq^7-4	jz^3-6	jz^3-7	y^3-1	s-1	Mitja
BuT1	11	1	2	4	3	5	2	5	0	3,67
BuT2	0	0	1	1	1	2	10	0	0	1,67
BuT3	18	5	5	8	13	6	5	8	4	8,00
BuT4	8	4	3	4	5	7	9	6	4	5,56
BuT5	29	11	31	22	46	27	20	19	2	23,00
BuT6	1	5	8	9	4	0	4	5	0	4,00
Galileo	50	46	64	62	62	62	52	54	53	56,11
Total	117	72	114	110	134	109	102	97	63	102

En els intervals de bandes (veure Taula 16) es comptabilitzen tants senyals com bandes hi ha incloses.

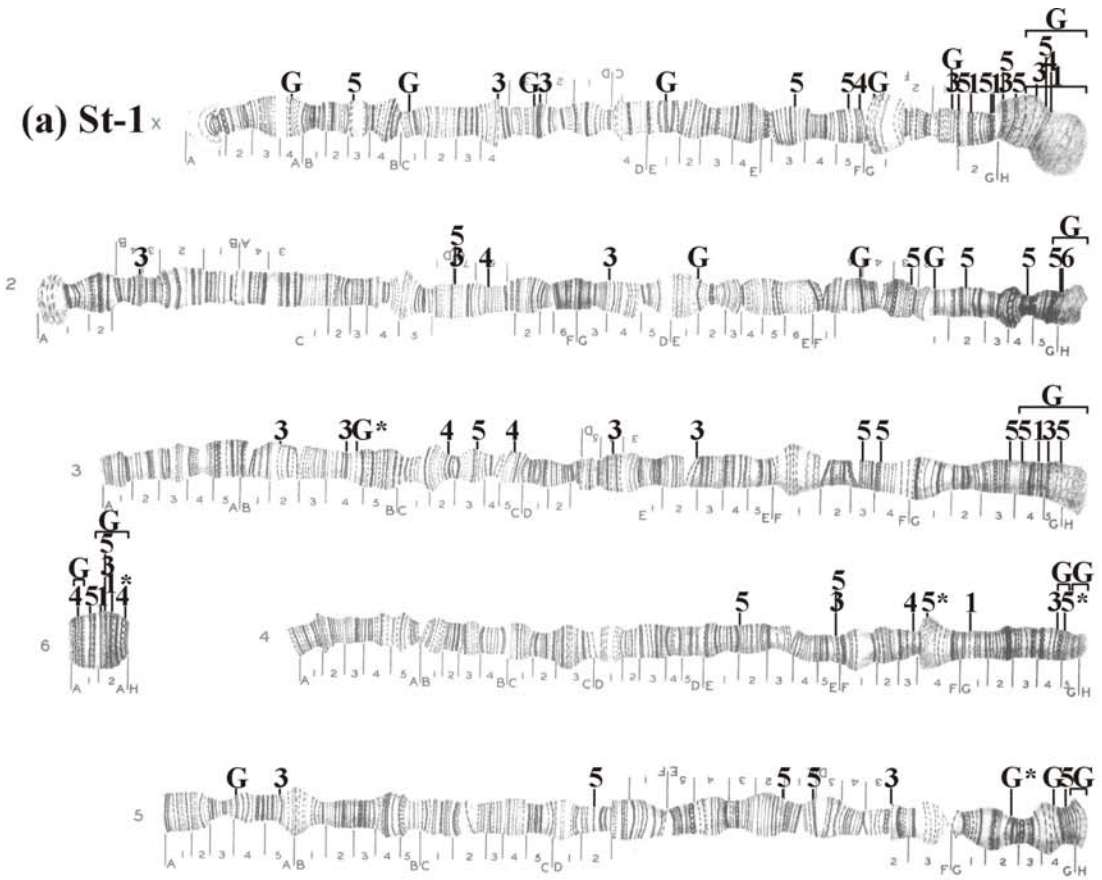
(a) St-1

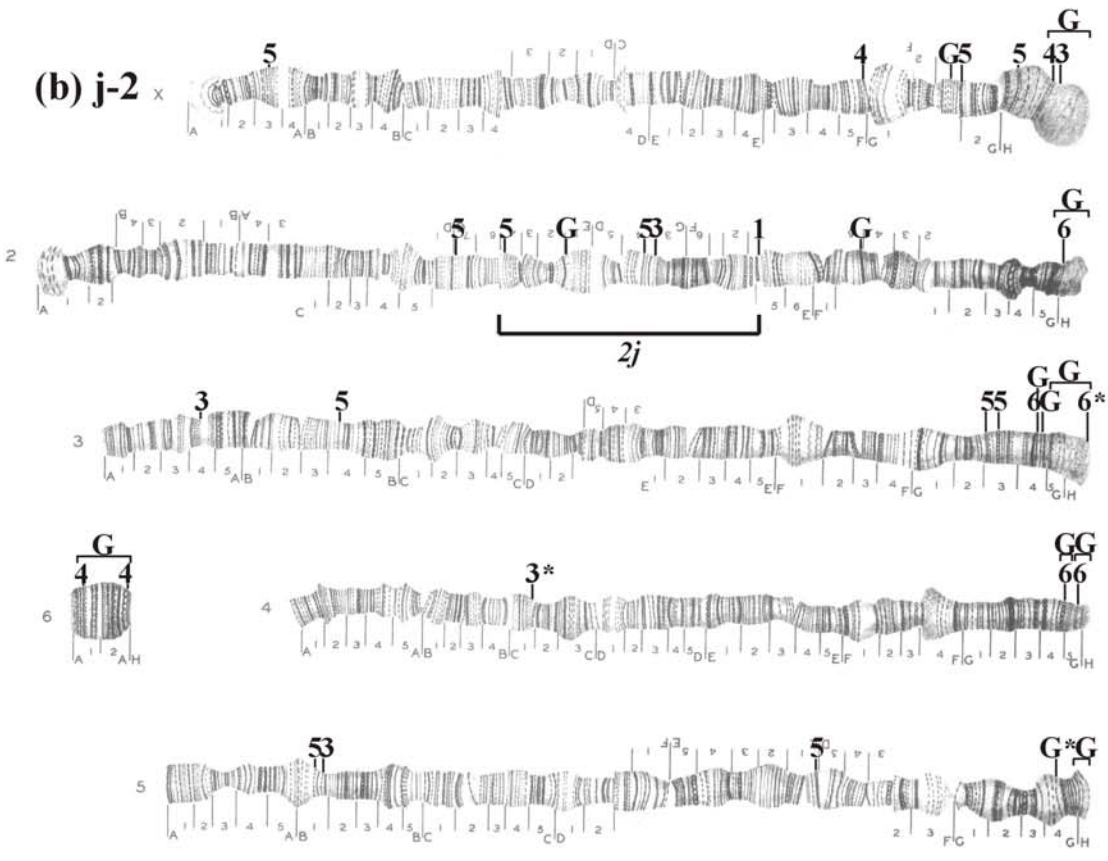
(b) j-2
2j

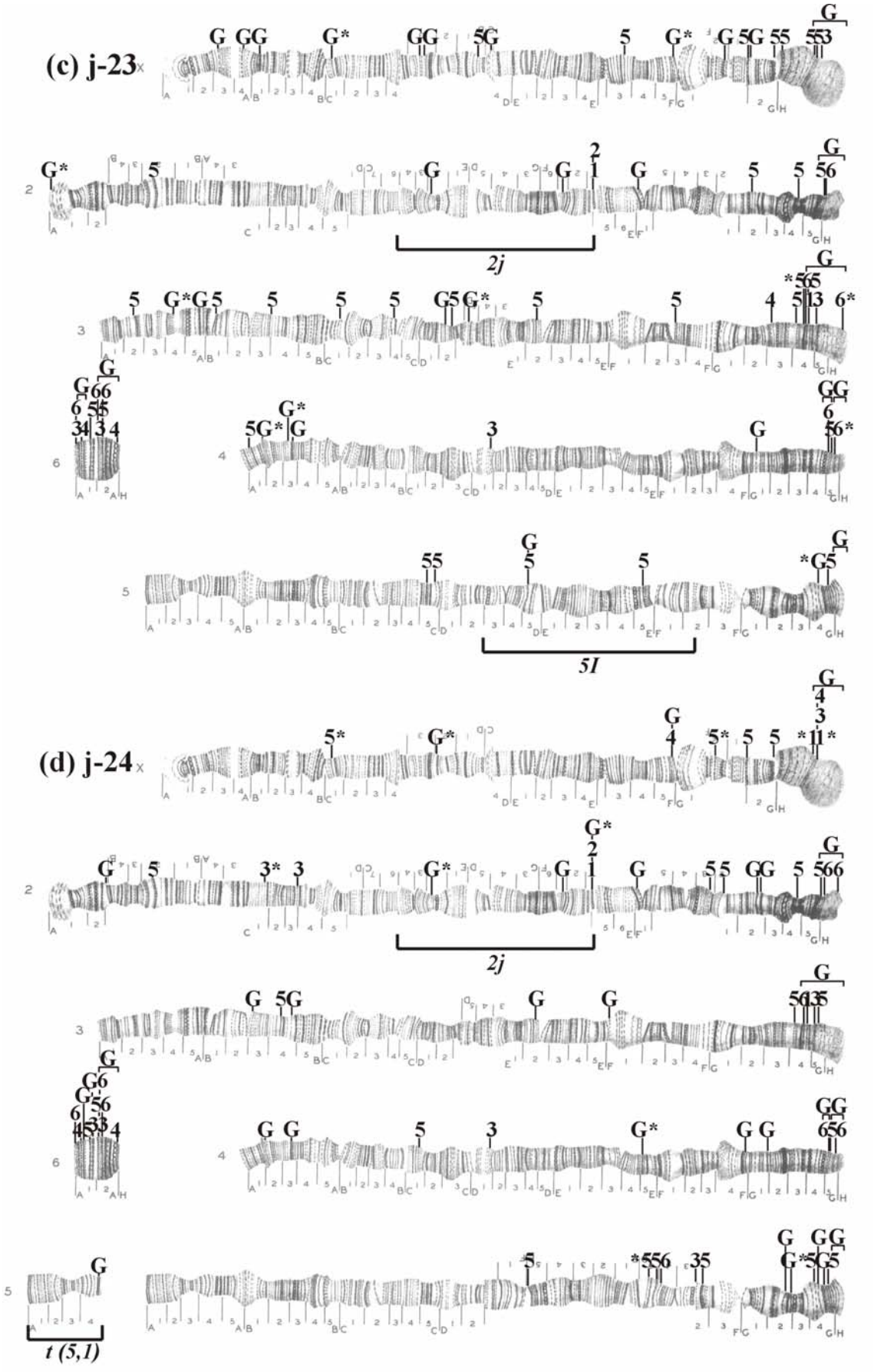
(c) j-23x
2j
51
(d) j-24x
2j
t (5,1)

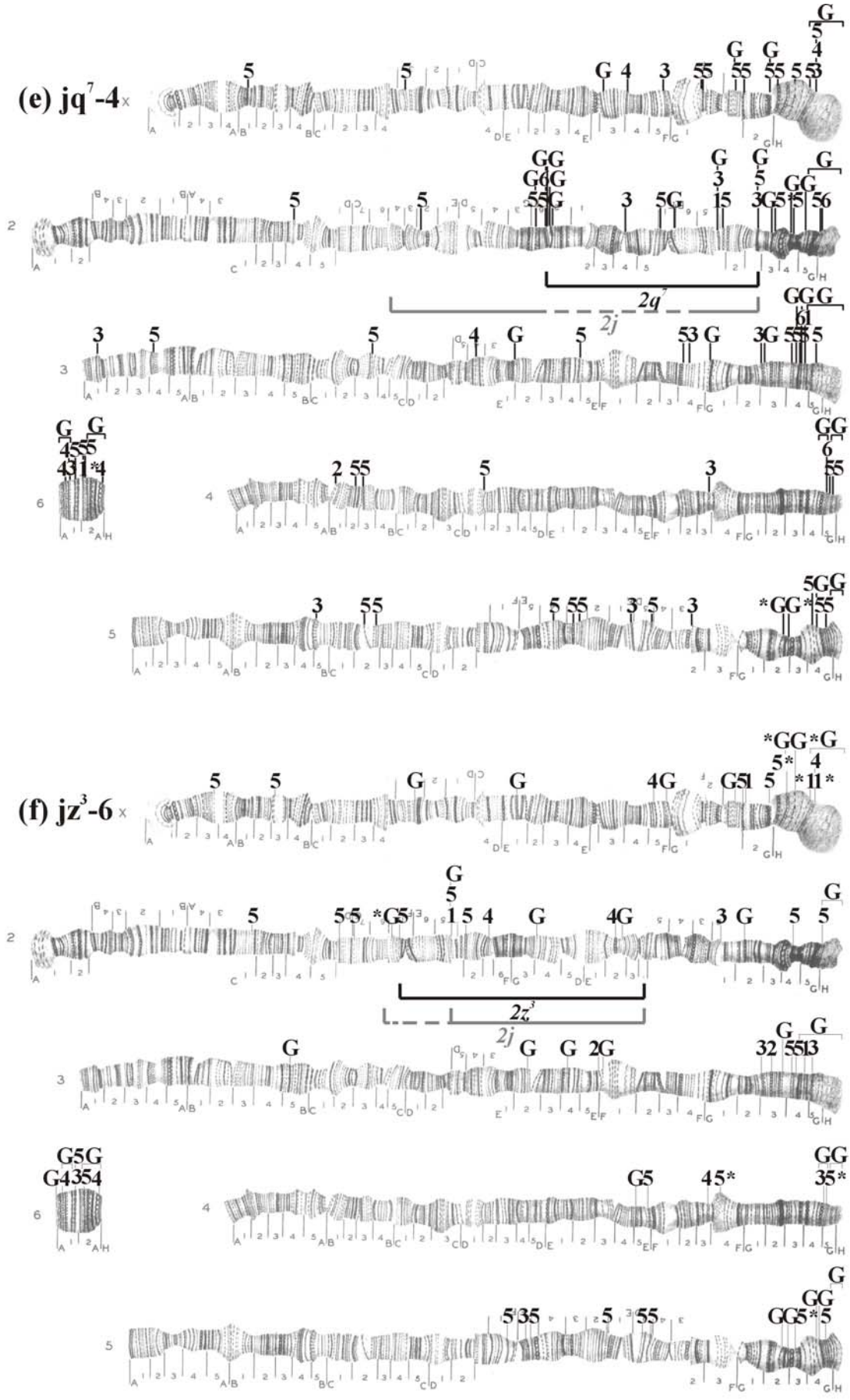
(e) jq7-4x
2q7
2j
(f) jz3-6x
2z3
2j

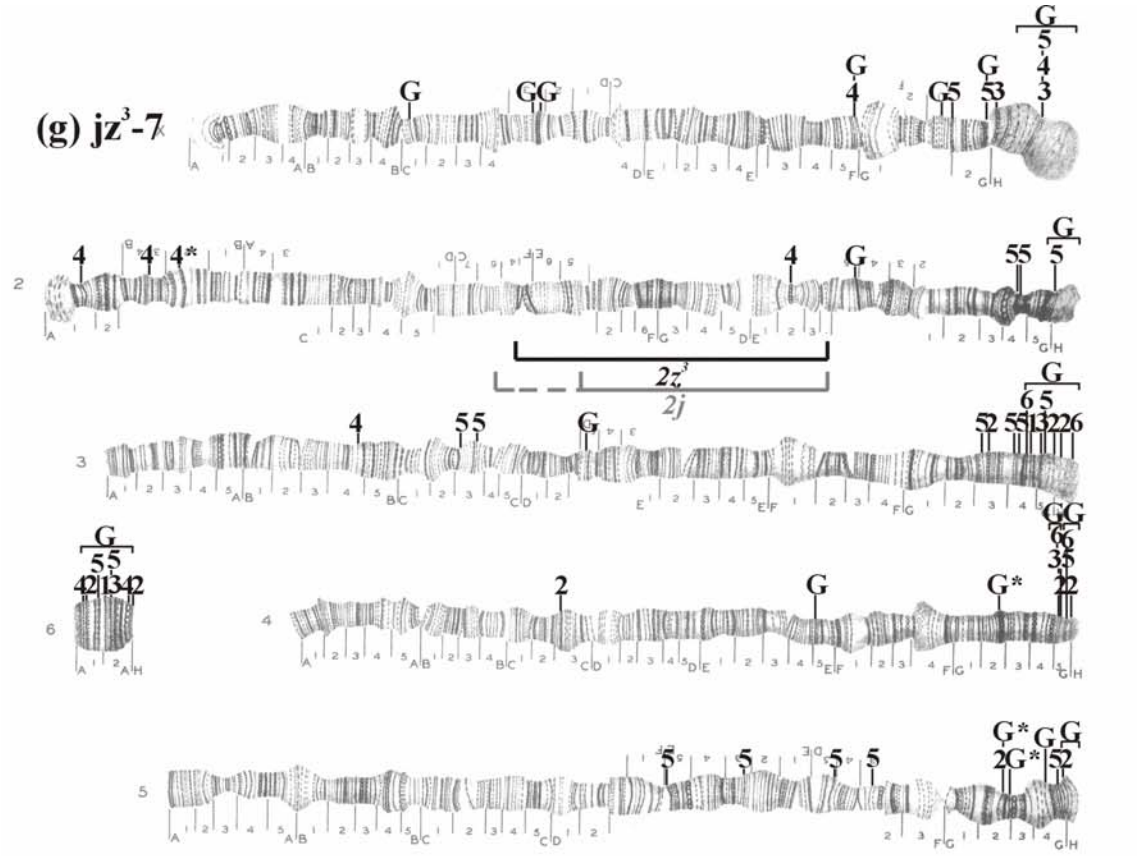
(g) jz³-7
2z³
2j

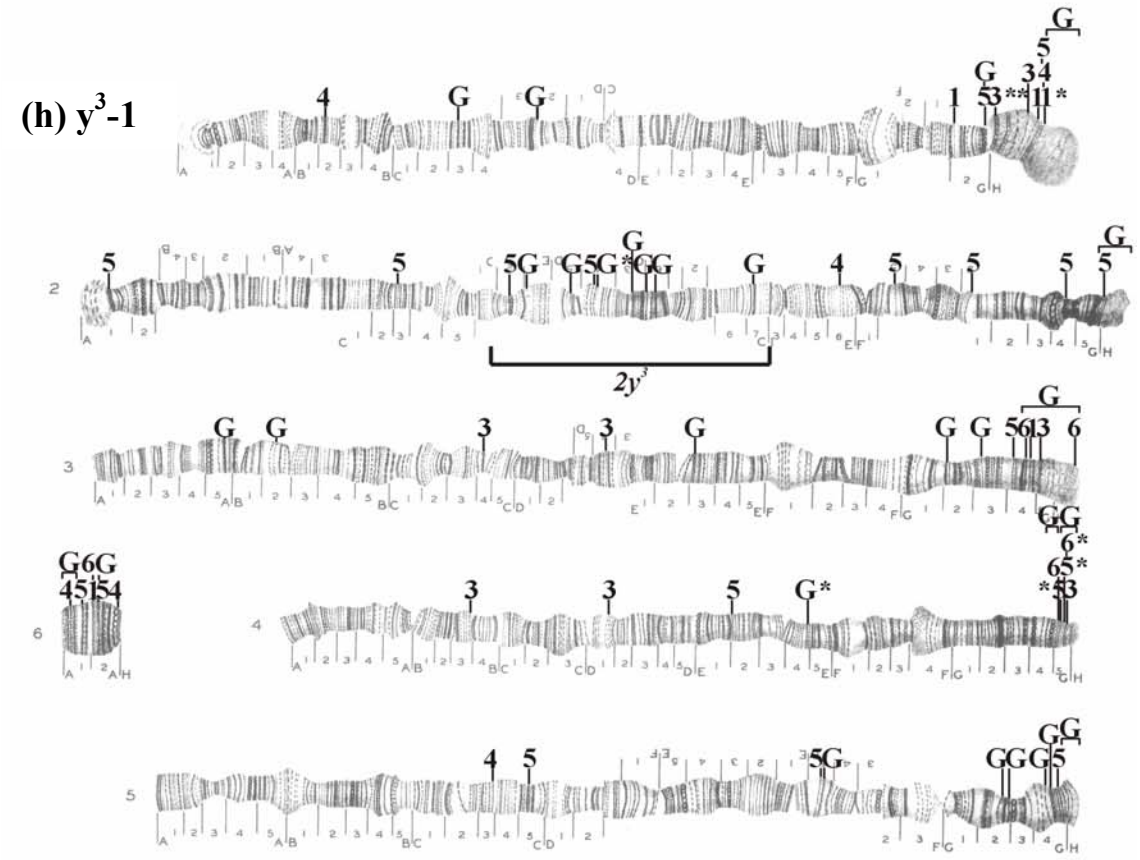
(h) y³-1
2y³

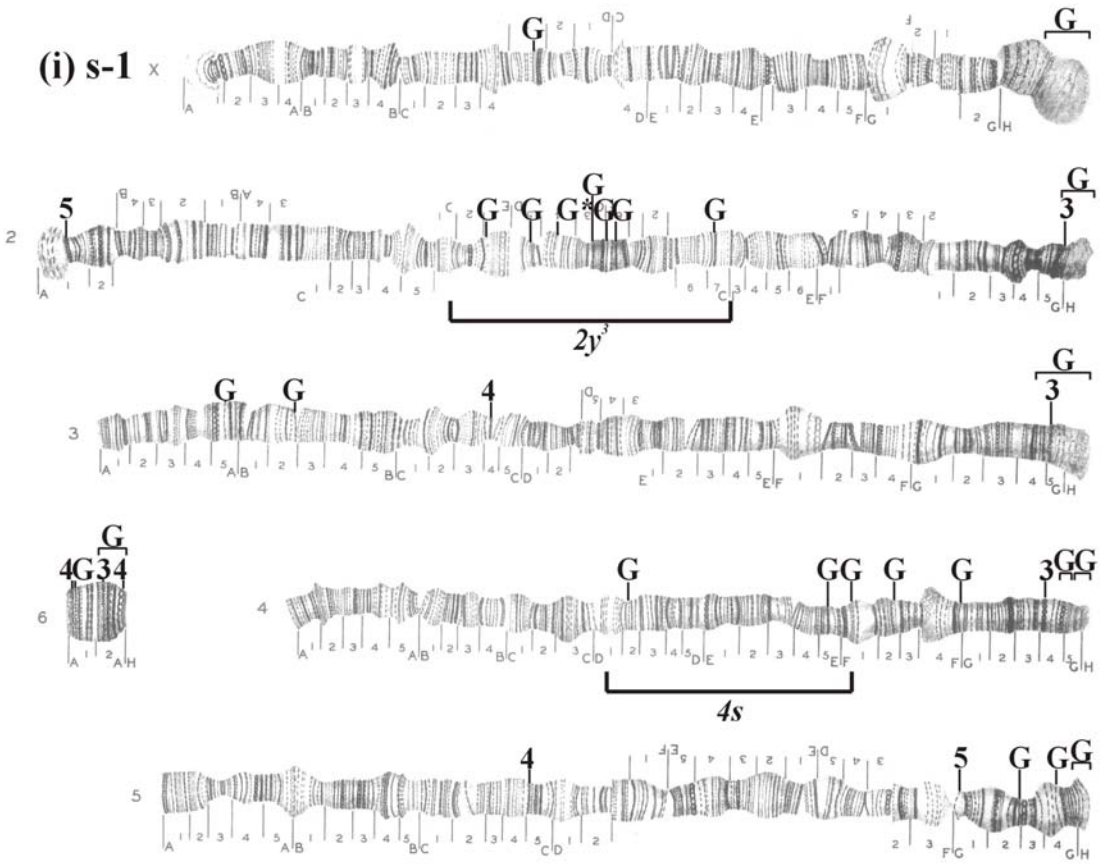

Figura 11. Senyals d'hibridació de *BuT1* (1), *BuT2* (2), *BuT3* (3), *BuT4* (4), *BuT5* (5), *BuT6* (6), i *Galileo* (G) sobre els cromosomes de les soques: (a) st-1, (b) j-2, (c) j-23, (d) j-24, (e) jq7-4, (f) jz3-6, (g) jz3-7, (h) y3-1, (i) s-1. S'indiquen les reordenacions cromosòmiques que presenta cada soca.

Taula 16. Localització dels elements transposables a les soques estudiades.

	BuT1	*BuT2*	*BuT3*	*BuT4*	*BuT5*	*BuT6*	*Galileo*
st-1	XG2d-e, XG2k, [XH1c-cen], 3G4f, 4G1c, 6A2a, 6A2e-f*.	-	XC4f, XD3b, XF1c, XH1a, XH1d, 2B4a, 2C7f, 2D4a, 3B2b, 3B4f, 3D4c, 3E2g, 3G5a, 4E5e, 4G4d, 5A5d, 5F2e, 6A2c	XF5g, XH1f, 2C6f, 3C2f, 3C5b, 4F3d, 6A1d, 6A2h	XB3b, XF3g, XF5d, XG2a, XH1g, XH1a, XH1b, XH1e, 2C7f, 2F3c, 2G2e, 2G4d, 2G5e-f, 3C3g, 3F3d, 3F4b, 3G3h, 3G4a, 3G5d, 4E2a, 4E5e, 4F4c, 4G4e*, 5D2d, 5E2a, 5E1a, 5G4g, 6A1g, 6A2c	2G5h	XA4b, XC1d, XD3d, XE1d, XG1b, XF1c, [XH1e-cen], 2E1g, 2F5a, 2G1e, [2G5e-cen], 3B4h*, [3G4a-cen], [4G4d-G5b], [4G5e-cen], 5A4a-b, 5G2f*, 5G4c, [5G4i-cen], [6 A1b-f], [6A1i-cen]
j-2	2E5a	-	XH1g, 2D4a, 3A4f, 4C1h*, 5B1g	XF5g, XH1f, 6A1d, 6A2h	XA3e-g, XG2a, XH1b, 2C7f, 2E4g, 2D4d, 3B4c, 3G3a, 3G3d, 5B1e, 5E1a	2G5h, 3G4e, 3H1a*, 4G4d, 4G5e	XF1c, [XH1e-cen], 2E1g, 2F5a, [2G5e-cen], 3G4e, 3G4f, [3G5a-cen], [4G4d-G5b], [4G5e-cen], 5G4c*, [5G4i-cen*], [6A1c-cen]
j-23	2E5a, 3G4f	2E5a	XH1g, 3G5a, 4D1f, 6A1a, 6A2a	3G3c, 6A1d, 6A2h	XD1c, XF3g, XG2a, XG2k, XH1a, XH1e, XH1f, 2B2d, 2G2e, 2G4d, 2G5e-f, 3A2d, 3B1d, 3B4a, 3C1e, 3C4b, 3D2g, 3E2e, 3F3d, 3G4a, 3G4d*, 3G4f, 4A1e, 4G5b, 5C5c, 5C5e, 5D5b, 5E5d*, 5G4g, 6A1g, 6A2c	2G5h, 3G4e, 3H1a*, 4G5a, 4G5e*, 6A1a, 6A2a, 6A2c	XA3c, XA4b, XB1f, XC1d*, XD3g, XD3e, XC4h, XF5g*, XF2b, XG2b, [XH1e-cen], 2A1a, 2E2g, 2D3e, 2F1c, [2G5e-cen], 3A4e*, 3A5e, 3D2d, 3D5d*, [3G4e-cen], 4A2a*, 4A3c*, 4A3d, 4G1c, [4G4d,-G5b], [4G5e-cen], 5D5b, 5G4c*, [5G4i-cen*] , [6A1b-f], [6A2b-cen]
j-24	XH1e*, XH1f*, 2E5a,3G4f	2E5a	XH1e, 2C1k*, 2C3f, 3G5a, 4D1f-g, 5F2e-f, 6A1i, 6A2a	XF5g, XH1f, 6A1d, 6A2h	XC1d*, XF2f*, XG2a, XG2k, 2B2d, 2F3c, 2F2a, 2G4d, 2G5e-f, 3B4d, 3G4a, 3G5b, 4C1e-f, 4G5b, 5E5h*, 5D5e*, 5D5b, 5F2g, 5G4b, 5G4g, 6A1g, 6A2c	2G5h, 2H1a, 3G4e, 4G5a, 4G5e, 5D4h, 6A1a, 6A2a, 6A2c	XD2i, XF5g, [XH1e-cen], 2A3a, 2E2f*, 2D3a, 2E5a*, 2F1c, 2G2g, 2G2h, [2G5e-cen], 3B3a, 3B4h, 3E2e, 3F1b, [3G4d-cen], 4A2a, 4A3d, 4E5a*, 4F4i, 4G1g, [4G4d-G5b], [4G5e-cen], 5G2f, 5G2h*, 5G4c, 5G4e, [5G4i-cen], 6A1e-f, 6A1i, [6A2a-cen], 5A4f(t 5,1)
jq7-4	2E5a, 3G4f, 6A2a*	4B1a	XF5e, XH1f, 2F4e, 2E5a, 2G2f, 3A1f-g, 3F4c-d, 3G3a, 4F3d, 5B5a, 5E1a, 5F2e, 6A1e-f	XF4a, XH1f, 3D4d-e, 6A1c-d, 6A2h	XB1f, XD3g-h, XG1g, XF1a, XF1c, XG2a, XG2k, XH1a, XH1c, XH1e, XH1f, 2C4c, 2E2g, 2G1g, 2D3c, 2F1h, 2D1h, 2G2f, 2G3e*, 2G4d, 2G5e-f, 3A4b, 3C3g, 3E4f, 3F4b, 3G4a, 3G4c, 3G4d, 3G5b, 4B2d, 4B3b, 4D1g, 4G5c, 4G5e, 5C2c, 5C2e, 5E4f, 5E3f, 5E3d, 5D5b, 5G4b, 5G4c, 5G4g, 6A1g, 6A2a, 6A2c	2D3c, 2G5h, 3G4e, 4G5a	XF3c, XF1c, XG2i-j, [XH1e-cen], 2G1g, 2D3c, 2G2e, 2G2d, 2G2c, 2F1a, 2E5a, 2G2f, 2G3d, 2G4c, 2G5b, [2G5c-cen], 3E1i, 3G1a, 3G3b, 3G4c, 3G4e, [3G4g-cen], [4G4d-G5b], [4G5e-cen], 5G2f*, 5G2h*, 5G4c, [5G4i-cen], [6A1a-f], [6A2c-cen]

jz3-6	XG2b, XH1e*, XH1f*, 2E5a, 3G4f	3F1a, 3G3d	2F2b, 3G3a, 3G5a, 4G5a, 5E5d, 6A1i	XF5c, XH1f, 2D3d, 2E2d, 4F3d, 6A1d, 6A2h	XA3k, XB3b, XG2a, XG2k, XH1b*, 2C1l, 2D1f, 2C7f, 2E4c, 2E5a, 2D2a, 2G4c, 2G5e-f, 3G4a, 3G4c, 4E5e, 4F4c*, 4G5b, 5F1b, 5E5c, 5E2a, 5D5e, 5D5b, 5G3b*, 5G4g, 6A1h, 6A2c	-	XD3d, XE1d, XF5g, XF1c, XH1b*, XH1c*, [XH1e-cen], 2E4g*, 2E5a, 2D4a, 2E2g, 2G2d, [2G5e-cen], 3B5c, 3E2e, 3E4c, 3F1b, 3G3h, [3G4d-cen], 4E5a, [4G4d-G5b], [4G5e-cen], 5G2f, 5G2h, 5G4c, 5G4d, [5G4i-cen], 6A1a, [6A1d-g], [6A2b-cen]
jz3-7	3G4f, 6A2a	3G3d, 3G5d, 3H1a, 4C3c, 4G5a, 4G5f, 5G2f, 5H1a, 6A1e, 6A2i	XH1a, XH1f, 3G5a, 4G5a, 6A2c	XF5g, XH1f, 2A1g, 2B3h, 2B2d*, 2E2d, 3B4h, 6A1d, 6A2h	XG2a, XG2k, XH1f, 2G4c, 2G4d, 2G5e-f, 3C3b, 3C3g, 3G3c, 3G4a, 3G4c, 3G5b, 4G5b, 5E5h, 5E3c, 5D5b, 5D3b-d, 5G4g, 6A1h, 6A2c	3G4e, 3H1a, 4G5a, 4G5e	XC1d, XD3d, XD3b, XF5g, XF1c, XG2k, [XH1c-cen], 2F5a, [2G5e-cen], 3D5d, [3G4e-cen], 4E5a, 4G2f*, [4G4d-G5b], [4G5e-cen], 5G2f*, 5G2h*, 5G4c, [5G4i-cen], [6A1b-d], [6A2c-cen]
y3-1	XG2b, XH1e*, XH1f*, 3G4f, 6A2a	-	XH1a*, XH1d, 3C4b, 3D4c, 3G5a, 4B3g, 4D1e, 4G5e	XB2b, XH1f, 2D6f, 5C3e, 6A1d, 6A2h	XG2k, XH1f, 2A1e, 2C3b, 2E2e, 2D4g, 2F5c, 2F2b, 2G4c, 2G5e-f, 3G4a, 4E2a, 4G5b*, 4G5d*, 5C5c, 5D5e, 5G4g, 6A1g, 6A2c	3G4e, 3H1a, 4G5a, 4G5e*, 6A2a	XC3a, XD3a, XG2k, [XH1g-cen], 2E1f, 2D5c, 2D4e-f*, 2D3e, 2F6i, 2F6f, 2C7b, [2G5e-cen], 3A5e*, 3B2c, 3E3a, 3G2a, 3G3c, [3G4d-cen], 4E4g-h*, [4G4d-G5b], [4G5e-cen], 5D5d, 5G2f, 5G2h, 5G4c, 5G4d, [5G4i-cen], [6A1a-f], 6A2c
s-1	-	-	2G5e, 3G5a, 4G4a, 6A2c	3C4b, 5C5b, 6A1c, 6A2h	2A2e, 5G1a	-	XD3d, [XH1e-cen], 2E1f, 2D5c, 2D4e-f, 2D3e, 2F6i, 2F6f, 2C7b, [2G5e-cen], 3A5c, 3B2f, [3G4e-cen], 4E5c, 4F1c, 4F2h, 4F4j, [4G4d-G5b], [4G5e-cen], 5G2h, 5G4c, [5G4i-cen], 6A1c-d, [6A2a-cen]

* senyals de menor intensitat.
Els intervals de bandes ([ ]) inclouen zones completament tenyides.
cen = centròmer.

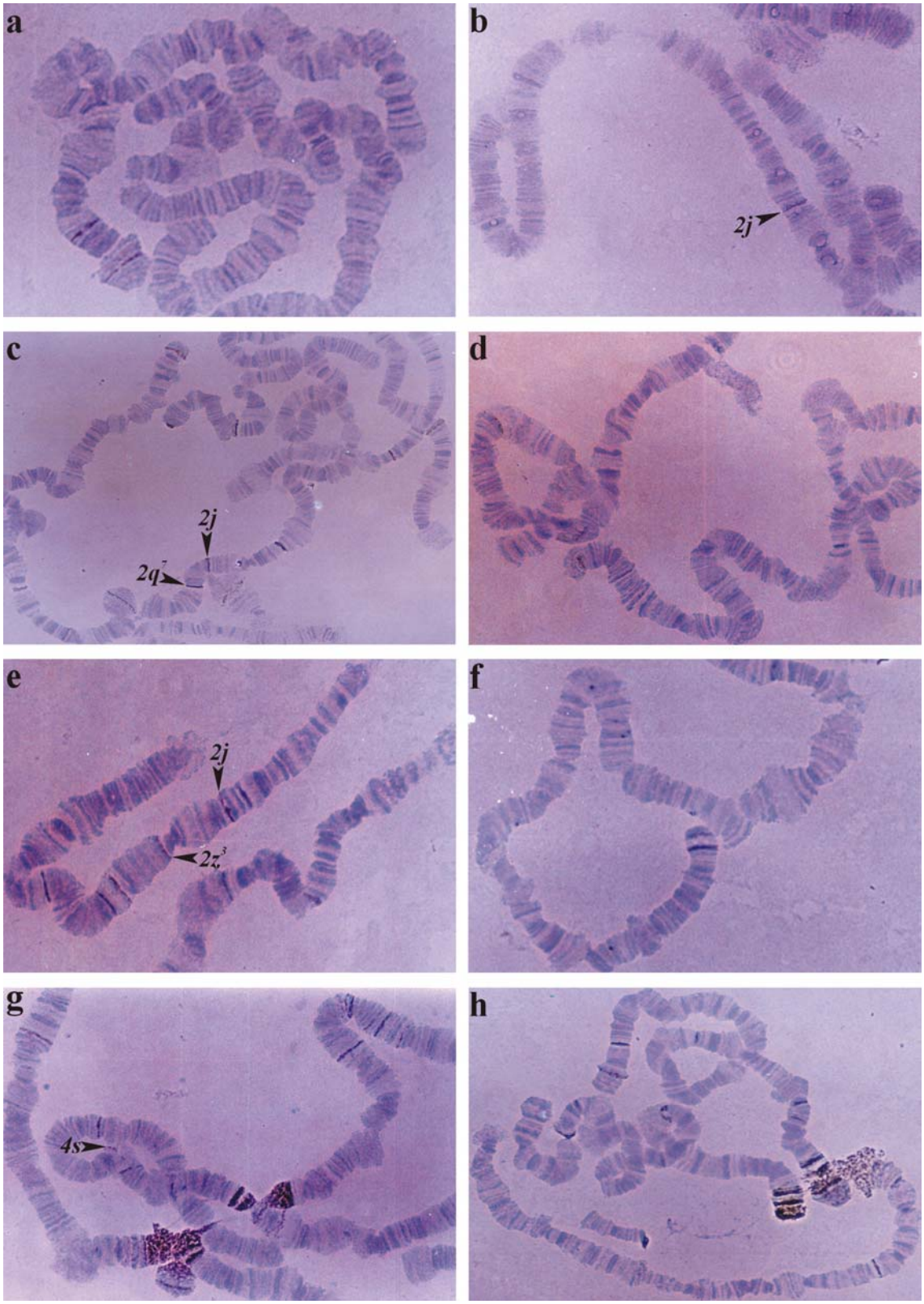

Figura 12. Senyals d'hibridació de: (a) *BuT1* sobre st-1, (b) *BuT2* sobre j-23, (c) *BuT3* sobre jq7-4, (d) *BuT4* sobre jz3-7, (e) *BuT5* sobre jz3-6, (f) *BuT6* sobre j-24, (g) *Galileo* sobre s-1, (h) *Galileo* sobre j-24. S'indiquen els senyals localitzats als punts de trencament d'inversions.

S'ha analitzat com es distribueixen els elements transposables entre els diferents cromosomes i dins dels cromosomes. La Taula 17 mostra el nombre d'elements observats i esperats en el sis cromosomes de *D. buzzatii*. Si els elements es reparteixen a l'atzar, el nombre d'insercions de cada cromosoma dependrà només de la seva mida. El percentatge del genoma que representa cada cromosoma s'ha calculat en funció del número de bandes segons el mapa de *D. repleta* (Wharton 1942). L'anàlisi de les dades de la Taula 17 mostra que els elements no es distribueixen a l'atzar entre els diferents cromosomes (χ^2 = 1368,21 g. l .= 5; P < 0,001). Aquestes diferències es deuen principalment a l'alt nombre d'insercions que hi ha al cromosoma 6. Tot i això, si s'elimina aquest cromosoma les diferències entre la resta de cromosomes segueixen sent significatives (χ^2 = 22,23; g. l .= 4; P < 0,001). Per últim, no s'han trobat diferències en el nombre d'insercions d'elements transposables entre el cromosoma X i els autosomes (χ^2 = 0,08; g. l .= 1; P = 0,774).

Taula 17. Número d'elements observats i esperats en els cromosomes de *D. buzzatii*.

Cromosoma	Nº de bandes	% del genoma	Nº d'elements observats	Nº d'elements esperats
X	234	19,0 %	151	174,42
2	286	23,2 %	171	212,98
3	240	19,5 %	196	179,01
4	223	18,1 %	139	166,16
5	231	18,8 %	110	172,58
6	18	1,5 %	151	13,77
Total	1.232	100%	918	918

Per analitzar si els elements transposables es distribueixen homogèniament en cada cromosoma s'han dividit els cromosomes, excepte el cromosoma 6, en tres parts (distal, central i proximal), i s'ha determinat si el nombre d'elements esperats en cada regió és diferent de l'observat (Taula 18). Les parts distal i proximal inclouen cadascuna el 10% de les bandes del cromosoma.

Taula 18. Distribució dels elements transposables en els cromosomes.

	Distal	Central	Proximal	Total	χ^2 (P)
Cromosoma X					
Observats	2	48	101	151	
Esperats	15,1	120,8	15,1	151	543,90 (**<0,001**)
Cromosoma 2					
Observats	5	86	80	171	
Esperats	17,1	136,8	17,1	171	258,80 (**<0,001**)
Cromosoma 3					
Observats	2	54	140	196	
Esperats	19,6	156,8	19,6	196	822,80 (**<0,001**)
Cromosoma 4					
Observats	6	33	100	139	
Esperats	13,9	111,2	13,9	139	592,81 (**<0,001**)
Cromosoma 5					
Observats	0	46	64	110	
Esperats	11	88	11	110	286,41 (**<0,001**)
Total					
Observats	15	267	485	767	
Esperats	76,7	613,6	76,7	767	2418,934 (**<0,001**)

Les regions distal, central i proximal dels cromosomes inclouen respectivament les següents bandes: X (A1a-A3g; A3h-G1c; F1e-H1g), 2 (A1a-A4f; B1a-G2c; G2d-H1a), 3 (A1a-A4a; A4b-G2d; G2e-H1a), 4 (A1a-A3d; A3e-G2d; G2e-H1a), i 5 (A1a-A3g; A3h-G2a; G2b-H1b). Els valors de probabilitat significatius s'escriuen en negreta.

Els resultats de la Taula 18 mostren que els elements no es distribueixen a l'atzar als cromosomes. Les regions distal i central mostren un dèficit d'elements respecte al número esperat, mentre que a la regió proximal dels cromosomes s'hi acumulen molts més elements dels esperats.